Circulation Research

ORIGINAL RESEARCH

Bone Marrow-Derived Cells Restore Functional Integrity of the Gut Epithelial and Vascular Barriers in a Model of Diabetes and ACE2 Deficiency

Yaqian Duan,* Ram Prasad,* Dongni Feng, Eleni Beli, Sergio Li Calzi, Ana Leda F. Longhini, Regina Lamendella, Jason L. Floyd, Mariana Dupont, Sunil K. Noothi, Gopalkrishna Sreejit, Baskaran Athmanathan, Justin Wright, Amanda R. Jensen, Gavin Y. Oudit, Troy A. Markel, Prabhakara R. Nagareddy, Alexander G. Obukhov, Maria B. Grant

RATIONALE: There is incomplete knowledge of the impact of bone marrow cells on the gut microbiome and gut barrier function.

OBJECTIVE: We postulated that diabetes mellitus and systemic ACE2 (angiotensin-converting enzyme 2) deficiency would synergize to adversely impact both the microbiome and gut barrier function.

METHODS AND RESULTS: Bacterial 16S rRNA sequencing and metatranscriptomic analysis were performed on fecal samples from wild-type, ACE2$^{-/y}$, Akita (type 1 diabetes mellitus), and ACE2$^{-/y}$-Akita mice. Gut barrier integrity was assessed by immunofluorescence, and bone marrow cell extravasation into the small intestine was evaluated by flow cytometry. In the ACE2$^{-/y}$-Akita or Akita mice, the disrupted barrier was associated with reduced levels of myeloid angiogenic cells, but no increase in inflammatory monocytes was observed within the gut parenchyma. Genomic and metatranscriptomic analysis of the microbiome of ACE2$^{-/y}$-Akita mice demonstrated a marked increase in peptidoglycan-producing bacteria. When compared with control cohorts treated with saline, intraperitoneal administration of myeloid angiogenic cells significantly decreased the microbiome gene expression associated with peptidoglycan biosynthesis and restored epithelial and endothelial gut barrier integrity. Also indicative of diabetic gut barrier dysfunction, increased levels of peptidoglycan and FABP-2 (intestinal fatty acid-binding protein 2) were observed in plasma of human subjects with type 1 diabetes mellitus (n=21) and type 2 diabetes mellitus (n=23) compared with nondiabetic controls (n=23). Using human retinal endothelial cells, we determined that peptidoglycan activates a noncanonical TLR-2 (Toll-like receptor 2) associated MyD88 (myeloid differentiation primary response protein 88)-ARNO (ADP-ribosylation factor nucleotide-binding site opener)-ARF6 (ADP-ribosylation factor 6) signaling cascade, resulting in destabilization of p120-catenin and internalization of VE-cadherin as a mechanism of deleterious impact of peptidoglycan on the endothelium.

CONCLUSIONS: We demonstrate for the first time that the defect in gut barrier function and dysbiosis in ACE2$^{-/y}$-Akita mice can be favorably impacted by exogenous administration of myeloid angiogenic cells.

VISUAL OVERVIEW: An online visual overview is available for this article.

Key Words: ACE2 ■ bone marrow ■ diabetes mellitus ■ microbiota ■ permeability

Meet the First Author, see p 934

The gut microbiome is increasingly becoming a major focal point for many inflammatory diseases because of its ability to regulate hematopoiesis and thus systemic inflammation. We previously demonstrated that modulation of the gut microbiome has long-lasting impact on diabetic retinopathy, a microvascular complication of diabetes

Correspondence to: Maria B. Grant, MD, Department of Ophthalmology and Visual Sciences, University of Alabama at Birmingham, 1670 University BLVD, VH490, Birmingham, AL 35294. Email mariagrant@uabmc.edu

*Y.D. and R.P. contributed equally to this article.

The online-only Data Supplement is available with this article at https://www.ahajournals.org/doi/suppl/10.1161/CIRCRESAHA.119.315743.

For Sources of Funding and Disclosures, see page 986.

© 2019 American Heart Association, Inc.

Circulation Research is available at www.ahajournals.org/journal/res

Downloaded from http://ahajournals.org by on August 26, 2021

Novelty and Significance

What Is Known?

- The gut microbiome can impact the pathogenesis of diabetes mellitus and its vascular complications.
- Diabetic vascular complications are associated with an imbalance in the renin-angiotensin system.
- Loss of ACE2 (angiotensin-converting enzyme 2) has a dramatic effect on hematopoiesis and intensifies the diabetes mellitus associated defect by reduced myeloid angiogenic cells (MACs) numbers and increasing myelopoiesis.
- Bone marrow changes precede the development of diabetic vascular complications.
- Microbial peptides can cause vascular damage.

What New Information Does This Article Contribute?

- In type 1 diabetic (Akita) mice, ACE2 deficiency promotes disruption of gut barrier integrity and results in the leakage of bacterial products into the circulation.
- Within the gut parenchyma, ACE2 deficient diabetic mice displayed reduced numbers of MACs without a concomitant increase in inflammatory monocytes.
- Exogenous administration of MACs restored both gut epithelial and vascular barriers and beneficially altered the microbiome by decreasing genes associated with peptidoglycan biosynthesis.
- In cultured endothelial cells, stimulation of TLR-2 (Toll-like receptor 2) failed to mediate NLRP3 inflammasome activation, and instead triggered noncanonical signaling by MyD88 (myeloid differentiation primary response protein 88)-ARNO (ADP-ribosylation factor nucleotide-binding site opener)-ARF6 (ADP-ribosylation factor 6), resulting in p120-catenin-mediated destabilization of adherens junctions and VE-cadherin internalization, increasing endothelial permeability.

In a mouse model of type 1 diabetes mellitus, ACE2 deficiency-induced defects in the gut barrier were not associated with increased inflammatory cells in the small intestine or with inflammasome activation of the vasculature. Rather, these defects in the gut barrier were associated with loss of the protective functions of MACs, a critical reparative bone marrow-derived population. In many disease processes that affect the gastrointestinal tract, including diabetes mellitus, the clinical emphasis has been on reducing inflammation; however, our findings suggest the need to assess changes in vascular reparative cells, such as MACs. In clinical trials that utilized MACs (typically $CD34^+$ cells in humans) for treatment of vascular dysfunction, the observed beneficial effect may have been due, in part, to the restoration of the gut barrier, beneficial changes in the gut microbiome, and reduced levels of toxic gut-derived peptides in the systemic circulation. This work provides rationale for directing future attention to changes in the gut barrier as an end point in clinical trials utilizing bone marrow populations. Such measurements can be easily evaluated by quantification of gut-derived peptides, such as peptidoglycan, or tight junction proteins, such as zonulin and FABP-2 (intestinal fatty acid-binding protein) in the serum before and after stem/progenitor cell administration.

Nonstandard Abbreviations and Acronyms

ACE2	angiotensin-converting enzyme 2
ARF	ADP-ribosylation factor 6
ARNO	ADP-ribosylation factor nucleotide-binding site opener
BM	bone marrow
ECFCs	endothelial colony-forming cells
FABP-2	intestinal fatty acid-binding protein 2
GVB	gut vascular barrier
HRECs	human retinal endothelial cells
IL	interleukin
MACs	myeloid angiogenic cells
MyD88	myeloid differentiation primary response protein 88
NK	natural killer
OTU	operational taxonomic unit
PV-1	plasmalemma vesicle-associated protein-1
SI	small intestine
T1D	type 1 diabetes mellitus
T2D	type 2 diabetes mellitus
TLR-2	Toll-like receptor 2
VEGF	vascular endothelial growth factor

mellitus,[1] by demonstrating that intermittent fasting in a mouse model of type 2 diabetes mellitus (T2D) increased levels of critical microbes that generated beneficial secondary bile acids, which were neuroprotective to the retina.

An imbalance of the renin-angiotensin system[2–9] has been implicated in the pathogenesis of vascular dysfunction. Reduction in the vasoprotective ACE2 (angiotensin-converting enzyme 2) results in loss of the vasoreparative functions of bone marrow (BM) cells,[10–12] thereby exacerbating various vascular complications, including diabetic

Downloaded from http://ahajournals.org by on August 26, 2021

retinopathy[11,13,14] Previously, we demonstrated that loss of ACE2 in the diabetic BM (*ACE2*$^{-/y}$-Akita mice) intensified the diabetic defect increasing myelopoiesis and the severity of diabetic retinopathy.[15]

BM cells, such as inflammatory monocytes, are known to migrate to the gut and impact gut function. In turn, the gut microbiota acts reciprocally to extrinsically regulate hematopoiesis.[16] Even very low levels of microbial antigens have the potential to set the size of the BM myeloid cell pool, which correlates strongly with the complexity of the intestinal microbiota.[17,18] Thus, recruitment of BM-derived immune cells to the gut plays a vital role in mediating and resolving inflammation.[17,19–21]

A subpopulation of BM-derived cells acts as a backup system for maintaining vascular homeostasis. This vascular reparative population was originally named endothelial progenitor cells due to their impact of endothelial health, but critical in vivo studies found that these cells did not directly differentiate into endothelial cells but rather provided their benefit strictly by paracrine secretion of growth factors and cytokines.[22–24] Based on this finding, they were renamed circulating angiogenic cells, and most recently, a consensus article regarding their nomenclature and phenotype called them myeloid angiogenic cells (MACs).[24] Despite discrepancies in nomenclature and phenotypic surface markers, human studies support an inverse correlation between the number of BM-derived vascular reparative cells and presence of atherosclerosis, adverse cardiovascular risk score, cardiovascular dysfunction, cardiovascular morbidity and mortality, and diabetic complications.[24–35] In addition to reduced numbers of MACs, the functional properties of these cells, such as cell adherence, migration, and tissue invasion, also seem to be attenuated in individuals with cardiovascular disease or diabetes mellitus. We demonstrated that loss of ACE2 in the diabetic BM (*ACE2*$^{-/y}$-Akita mice) reduced MAC number and function.[15] However, little is known about the role of BM derived-vascular reparative cells, such as MACs, on gut vasculature and gut barrier function.

We hypothesized that exogenous administration of MACs could provide trophic support to the gut epithelium and the gut vascular barrier (GVB), restoring the integrity of these 2 barriers and preventing leakage of harmful gut microbial peptides into the systemic circulation. We found that MAC treatment not only restored the GVB and gut epithelial barrier but beneficially impacted gut dysbiosis.

METHODS

Detailed methods are available in the Online Data Supplement section. The data, analytical methods, and other study materials will be provided upon reasonable request to the corresponding author.

Study Design

The objective of our study was to examine how the combined effects of type 1 diabetes mellitus (T1D) and ACE2 deficiency impact gut barrier function and the gut microbiome. Fecal samples, blood, and small intestine (SI) were obtained from Akita and *ACE2*$^{-/y}$-Akita mice at 9 months of diabetes mellitus as well as age- and gender-matched wild-type (WT) and *ACE2*$^{-/y}$ mice to study microbiota composition and gut barrier function. Following the characterization of the cell populations that were altered by the presence of T1D and ACE2 deficiency within the intestine, we corrected these deficiencies by exogenous replacement of cells obtained from WT mice and then assessed the impact of cell administration on gut barrier function and the microbiome. In vitro experiments were performed to examine the mechanisms of endothelial activation by microbial peptides such as peptidoglycan released from the gut into the circulation.

Animals

WT (genotype: *ACE2*$^{+/y}$-*Ins2*$^{WT/WT}$), Akita (genotype: *ACE2*$^{+/y}$-*Ins2*$^{WT/C96Y}$), *ACE2* knockout (*ACE2*$^{-/y}$; genotype: *ACE2*$^{-/y}$-*Ins2*$^{WT/WT}$), and *ACE2*$^{-/y}$-Akita (genotype: *ACE2*$^{-/y}$-*Ins2*$^{WT/C96Y}$) mice were utilized for these studies. The *ACE2*$^{-/y}$ mouse strain was originally obtained from Dr Gavin Oudit (University of Alberta, Canada).[13] The *Ins2*$^{WT/C96Y}$ mouse strain was purchased from the Jackson Laboratory (Bar Harbor, ME). All mice were on a C57BL/6 genetic background. The Akita strain is a monogenic model for phenotypes associated with T1D. Heterozygous Ins2Akita mice (*Ins2*$^{WT/C96Y}$) develop insulin-dependent diabetes mellitus, including hyperglycemia, hypoinsulinemia, polydipsia, and polyuria by 3 to 4 weeks of age. The phenotype is more severe in males than in females. Therefore, only age-matched male mice were used in this study and were not assigned randomly but rather assigned based on genotype. To generate the *ACE2*$^{-/y}$-Akita (*ACE2*$^{-/y}$/*Ins2*$^{WT/C96Y}$) male mice, female heterozygous *ACE2*$^{-/+}$ mice were bred with male heterozygous *Ins2*$^{WT/C96Y}$ mice at Indiana University School of Medicine (IACUC no. 11165) and University of Alabama (IACUC no. 21196). The metabolic phenotype of the WT, Akita, *ACE2*$^{-/y}$, and *ACE2*$^{-/y}$-Akita mice has been previously published.[15] For each experiment, mice from each cohort had a metabolic evaluation (fasting blood glucose and glycated hemoglobin) to confirm that the WT & *ACE2*$^{-/y}$ were euglycemic and that the diabetic Akita & *ACE2*$^{-/y}$-Akita cohorts had a similar degree of diabetes mellitus (glucose intolerance). Only healthy-appearing mice were used for this study and any mouse that exhibited evidence of illness, such as excessive wasting or lethargy, was excluded.

Experimental mice were housed in closed cages (up to 5 mice per cage) under a 12-hour/12-hour light-dark cycle. Cages were not stacked to prevent fecal contamination. A polymerase chain reaction (PCR) approach was used to identify the *ACE2*$^{-/y}$ and heterozygous Akita mice by using mouse tissue obtained during ear biopsies. The following primers were used: *ACE2* gene genotyping: forward—CCG GCT GCT CTT TGA GAG GAC A and reverse—CTT CAT TGG CTC CGT TTC TTA GC; *ACE2*$^{-/y}$ mouse genotyping: forward—CCG GCT GCT CTT TGA GAG GAC A and reverse—CCA GCT CAT TCC TCC CAC TC; Akita mouse genotyping: forward—TGC TGA TGC CCT GGC CTG CT and reverse—TGG TCC CAC ATA TGC ACA TG. For Akita mice genotyping, restriction digestion was performed using Fnu4HI after PCR.

16S rRNA Gene Sequencing

The stool samples were obtained while holding the mice in the air and collected directly into sterile DNA/RNA free Eppendorf tubes (1.5 mL) to minimize any contamination. Immediately

Downloaded from http://ahajournals.org by on August 26, 2021

after collection of fecal samples, tubes were tightly closed, sealed with paraffin, frozen within 10 minutes at −80°C, and stored in a −80°C freezer. These frozen fecal samples were shipped to Wright Labs, LLC, for the 16S rRNA sequencing (V3–V4 region) and metatranscriptomic analysis. Genomic DNA was extracted (≈0.25 µg per sample) using a MoBio Powerfecal DNA Isolation kit following the manufacturer's instructions (MoBio Carlsbad, CA). The Disruptor Genie cell disruptor (Scientific Industries, Bohemia, NY) was used to vortex the samples. The isolated genomic DNA was then eluted in 50 µL of 10 mmol/L Tris and quantified using the Qubit 2.0 (Invitrogen) Fluorometer according to the protocol of the dsDNA high-sensitivity option. PCR was performed using 10 ng of template DNA at a total volume of 25 µL per reaction. After PCR amplification, the products were then purified using the Qiagen Gel Purification Kit (Qiagen, Frederick, MD). After quality check using the 2100 Bioanalyzer DNA 1000 chip (Agilent Technologies, Santa Clara, CA), pooled libraries were then shipped to California State University (North Ridge, CA) for sequencing. After quantification using the Qubit High Sensitivity dsDNA kit (Life Technologies, Carlsbad, CA) and dilution, pooled libraries were loaded on an Illumina MiSeq V2 500 cycle kit cassette with 16S rRNA library sequencing primers and set for 250 base pair, paired-end reads. Raw sequence data were successfully obtained; paired-end sequences were trimmed at a length of 250 bp, and quality control was set as an expected error of <0.005 by USEARCH V7. Reads were then analyzed by the QIIME 1.9.0 software. The USEARCH61 algorithm was used to identify chimeric sequences and to pick open reference operational taxonomic units (OTUs). Taxonomy was assigned using the Greengenes 16S rRNA gene database (13–5 release, 97%) and organized into a BIOM formatted OTU table, which was summarized within QIIME 1.9.0. Singletons and doubletons were removed from the dataset before the initiation of any diversity analysis.[36] The full report and statistical analysis from Wright Labs, Huntingdon, PA, is available upon request.

α-Diversity Analysis

The plots of α-diversity were generated within the QIIME-1.9.0 sequence analysis package using multiple rarefactions to a maximum sequencing depth of 27 000 sequences per sample at a step size of 2700 with 20 iterations at each step. α-diversity plots were generated using the observed species richness metric.

β-Diversity Analysis

ANOSIM significance tests and principal coordinates analysis plots were generated from a weighted UniFrac distance matrix from a CSS (cumulative sum scaling) normalized OTU table within QIIME 1.9.0. The data were then uploaded to the online analysis tool METAGENassist for PLS-DA (partial least squares-discriminant analysis) analysis. Principal coordinates analysis was conducted for the 16S rRNA data set (fecal samples).

Taxonomic Comparisons

BIOM formatted OTU table was used to organize assigned taxonomy. To identify the abundance of prevalent phyla, facet grid bar plots were generated within Rstudio using the Phyloseq package.

LefSe Analysis

Relative abundances of taxa were multiplied by 1 million and formatted as described before.[37] Comparisons were made with sample type as the main categorical variable (class). α levels of 0.05 were used for both the Kruskal-Wallis and pairwise Wilcoxon tests. Linear discriminant analysis scores >3.0 are displayed.

Metatranscriptomic Analysis of Fecal Samples

Fecal samples (n=39) underwent MoBio (Qiagen, CA) RNA extraction. Subsequent Nugen Ovation (Nugen, CA) transcriptome library was prepared for all fecal samples, and the quality of the library was checked using a high-sensitivity bioanalyzer chip (Agilent, CA). Then, the library was purified using the QIAquick gel purification kit (Qiagen, CA) after equimolar amounts were pooled. After purification, libraries underwent sequencing on the Illumina HiSeq4000 following a 2×150 index run. Quality assessment of the raw sequencing data was performed using the program FastQC. A sliding window filtration within the program trimmomatic was used to filter the sequence data; then human DNA reads were also removed from the filtered sequence data. The metatranscriptome analysis tool metaphlan was implemented to quantify the taxonomic profile within each sample. To obtain functional gene profiles, filtered data were annotated using the Uniref90 database within Humann2. Uniref90 annotations were regrouped as KEGG (Kyoto Encyclopedia of Genes and Genomes) orthology terms, which consequently underwent counts per million normalization within Humann2 for stratified barplot analysis and LefSe enrichment plots. Functional count data were also uploaded to the online analysis tool METAGENassist for PLS-DA analysis.

Flow Cytometry Analysis

Isolated cells were incubated with rat anti-mouse CD16/CD32 (eBioscience, San Diego, CA) for 15 minutes at 4°C. The cells were then incubated with primary antibody cocktails for 30 minutes at 4°C in the dark (for myeloid angiogenic cells, Alexa700 anti-mouse CD45, Catalog no. 560510, BD Biosciences, San Jose, CA; BV650 anti-mouse Flk-1, Catalog no. 740539, BD Biosciences; PerCP-eFluor710 anti-mouse CD31, Catalog no. 46-0311-82, eBioscience). Immune cells and monocytes were identified after staining with the following antibodies: PerCPCy5.5 anti-mouse natural killer (NK) 1.1, Catalog no. 551114, BD Biosciences; BV500 anti-mouse CD3, Catalog no. 560771, BD Biosciences; PE/Cy7 anti-mouse CD11c, Catalog no. 558079, BD Biosciences; PE anti-mouse Ly6G, Catalog no. 551461, BD Biosciences; BV421 anti-mouse CD115, Catalog no. 135513, Biolegend, San Diego, CA; fluorescein isothiocyanate anti-mouse Ly6C, Catalog no. 128006, Biolegend). After washing, the cells were then stained with flexible viability dye eFluor 780 (Catalog no. 65-0865-18, eBioscience) for 30 minutes at 4°C, washed with PBS twice, then fixed with 1% paraformaldehyde for flow cytometry.

BM-Derived CD45$^+$CD31$^+$Flk-1$^+$ Cell Sorting and Injection

BM of C57/BL/6 mice (n=15) was collected, pooled, and stained with antibodies against CD45-APC, Flk-1-PerCPCy5.5,

Downloaded from http://ahajournals.org by on August 26, 2021

and CD31-BV421 (BD Biosciences, CA). Triple positive cells were sorted using BD FACSAria IIu and frozen in 30% fetal bovine serum supplemented with 10% dimethyl sulfoxide (DMSO) at a cell density of 4×10^5 cells/mL. Fifty thousand BM $CD45^+CD31^+Flk\text{-}1^+$ cells in 200 µL PBS were delivered every other day for 6 days via intraperitoneal injection into mice from each of the 4 cohorts. Mice from each of the 4 cohorts were injected with 200 µL PBS and were considered experimental control groups. Then, mice were euthanized for tissue harvesting 7 days following the first intraperitoneal injection of stem cells.

Human Retinal Endothelial Cell Culture and Treatment Conditions

Human retinal endothelial cells (HRECs) were obtained from Cell Systems (Kirkland, WA). HRECs were cultured and maintained in classic cell culture medium (Cell Systems) supplemented with 10% fetal bovine serum and 2% animal-derived growth factors at 37°C in a 95% humidified incubator with 5% CO_2. Only low-passage HRECs (<6–9 passages) were used in the described experiments. Approximately 50 000 cells/well were seeded onto the chambered slides and allowed to grow in culture until reaching 80% to 90% confluence. TLR-2 (Toll-like receptor 2), MyD88 (myeloid differentiation primary response protein 88), ARNO (ADP-ribosylation factor nucleotide-binding site opener), ARF6 (ADP-ribosylation factor 6), and p120-catenin staining was preformed when the cells reached 100% confluence. Purified peptidoglycan from *Staphylococcus aureus* (No. 77140, Sigma-Aldrich, St Louis, MO) and NAV2729, an inhibitor of ARF6 (No. 5986, Tocris Bio-Techne Corporation, Minneapolis, MN), were used to determine the role of peptidoglycan on vascular permeability. HRECs were treated with peptidoglycan in a dose-dependent manner (40 and 100 µg/mL) for 24 hours. In select experiments, HRECs were pretreated with NAV2729 (10 µmol/L) for 1 hour followed by peptidoglycan treatment for 24 hours. The peptidoglycan and NAV2729 were dissolved in DMSO before adding to the culture medium. The final concentration of DMSO in the culture medium did not exceed 0.1% (v/v), and an equivalent amount of DMSO was added to the culture media of control (untreated) groups.

Data Analysis and Statistics

Power calculation was performed to estimate sample size required to demonstrate a significant reduction in either endothelial or epithelial gut permeability in the Akita and $ACE2^{-/y}$-Akita mice compared with WT. We estimated that a minimum of 6 mice would be necessary to demonstrate a statistically significant difference in immunohistochemistry staining intensity with a power of 80% and an error α of 5% (2 sided) assuming a change of 50% in the expression of the immunohistochemistry markers of leakage in the Akita and $ACE2^{-/y}$-Akita cohorts compared with WT. Due to the diabetic condition, we observed 50% to 60% mortality in Akita and $ACE2^{-/y}$-Akita mice, which reduced the n number of samples to 3 at some end points.

Data were evaluated for normal distribution using GraphPad Prism, version 8.1 software. For multigroup comparisons of normally distributed data, 1-way ANOVA was performed followed by an appropriate post hoc *t* test. Student *t* test was used for comparison among 2 groups. Multiple testing was done only within tests but not across all tests. The nonparametric Kruskal-Wallis and pairwise Wilcoxon tests were used for microbiota LefSe enrichment analysis. The data sets were considered significantly different if the *P* was <0.05. Box and whiskers plots are shown for each data set. Multiple permutations (1000) were conducted for ANOSIM and PERMANOVA analysis of β-diversity clustering between cohorts, as well as all α-diversity pairwise comparisons.

RESULTS

Loss of ACE2 Alters the Microbiota Composition and the Functional Profile in Diabetic Mice

To investigate whether ACE2 deficiency affects the composition of the gut microbiota in diabetes mellitus, fecal samples from $ACE2^{-/y}$-Akita and Akita mice at 9-month of diabetes mellitus, as well as their age-matched controls ($ACE2^{-/y}$ and WT mice), were collected and examined by 16S rRNA gene sequencing. α-diversity (an indicator of species richness), the number of different species in a sample, or the number of distinguishable taxa (OTU's) in each sample, revealed a significant increase in WT mice when compared with $ACE2^{-/y}$ (P=0.036) and Akita (P=0.006) mice (Figure 1A). Differences in α-diversity between WT and $ACE2^{-/y}$-Akita mice were not statistically significant. $ACE2^{-/y}$-Akita mice were found to yield a significantly increased mean observed species measure when compared with Akita mice (P=0.030).

β-diversity was used to measure the phylogenetic distance between the bacterial community in each sample (Figure 1B through 1D). In Figure 1B through 1D, principal coordinates analysis for the 16S rRNA data set is shown. Each point on the plot is indicative of the entire bacterial community within a sample. Samples that are closer together share similar microbial community makeup, whereas samples that are further apart are less similar. We observed that each genotype exhibited a distinct clustering of bacterial taxa in the fecal samples collected, suggesting both ACE2 deficiency and diabetes mellitus lead to an alteration of the gut microbiota composition. The principal coordinates analysis demonstrates significantly differential clustering between genotypes when considering the ANOSIM (P=0.002) and PERMANOVA (P=0.001) test statistics.

Figure 1E shows a heat map of bacterial counts per million normalized to counts of Metaphlan, producing estimated taxonomic read hits and generating a visualized difference in prominent taxa among different groups. A LefSe plot was then generated to display enriched functional gene pathways (MetaCyc) expressed within each respective genotype cohort (Figure 1F). Interestingly, the $ACE2^{-/y}$-Akita cohort appeared to have the most defined functional expression profile. When compared with Akita mice, 2 major functional pathways found in the $ACE2^{-/y}$-Akita mice were involved in peptidoglycan biosynthesis

Downloaded from http://ahajournals.org by on August 26, 2021

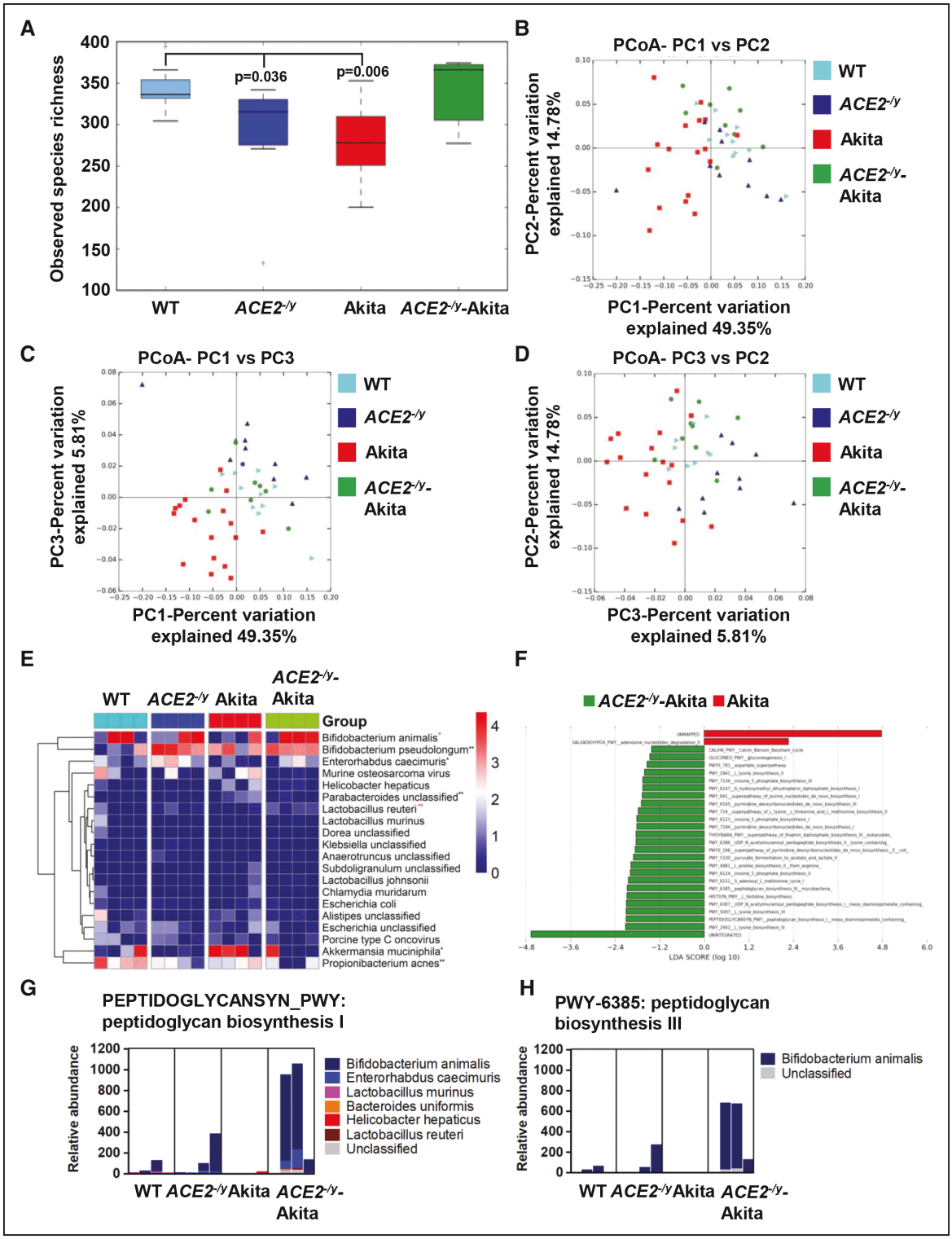

Figure 1. ACE2–/*y*-Akita exhibited distinct microbiota and functional profiles and was enriched in peptidoglycan biosynthesis pathways in its fecal samples.

A, α-diversity boxplots compared the observed species richness between microbiome samples from all 4 genotypes and revealed a significant decrease in *ACE2*$^{-/y}$ (*P*=0.036) and Akita (*P*=0.006) mice compared with wild type (WT); however, the *ACE2*$^{-/y}$-Akita cohort was not significantly different from WT (n=4). **B–D**, Two-dimensional principal coordinates analysis (PCoA) plots of weighted UniFrac distancs reveal significantly differential phylogenetic community compositions within each genotype (anosim *P*=0.002) and PERMANOVA (*P*=0.001; n=9 WT; 10 *ACE2*$^{-/y}$; 17 Akita; and 9 *ACE2*$^{-/y}$-Akita). **E**, A heat map of counts per million (CPM) normalized counts of metaphlan displayed differential abundances of several prominent taxa (n=4). **F**, Increased functional pathways of peptidoglycan biosynthesis in *ACE2*$^{-/y}$-Akita mice compared with Akita mice by LefSe plots (linear discriminant analysis score >2). **G** and **H**, *Bifidobacterium animalis* is the main bacterial taxa that are responsible for peptidoglycan (PGN) biosynthesis.

Downloaded from http://ahajournals.org by on August 26, 2021

(Figure 1G and 1H). The other 2 most abundant pathways were involved in the biosynthesis of L-lysine, a vital component of the amino acid chain of peptidoglycan (Online Figure IA and IB). Moreover, the loss of ACE2 resulted in an enrichment of the pathway that mediates biosynthesis of the peptidoglycan precursor, UDP-N-acetylmuramoyl pentapeptide (Online Figure IC). Interestingly, when comparing WT and *ACE2*$^{-/y}$ samples, only 2 functional gene pathways were found to be enriched within *ACE2*$^{-/y}$ samples (not displayed), whereas zero pathways were found to be significantly enriched within WT samples. Both starch degradation V and tetrapyrrole biosynthesis from glutamate metacyc pathways were significantly (linear discriminant analysis> 1.0, P=0.05) enriched within *ACE2*$^{-/y}$ samples when compared with WT (not displayed). When considering the difference between WT and Akita, we observed an increase in gene expression for S-adenosyl L-methionine cycle, L-lysine, L-threonine and L-methionine biosynthesis, and L-proline biosynthesis, whereas in the Akita there was a reduction in chorismate biosynthesis, L-arginine biosynthesis, aromatic amino acid biosynthesis, and dTDP L-rhamnose biosynthesis (Online Figure IIA). When considering the difference in functional gene expression between WT and *ACE2*$^{-/y}$-Akita samples, 40 significantly enriched functional pathways were identified in *ACE2*$^{-/y}$-Akita samples, whereas there were no pathways identified to be significantly enriched within WT samples (Online Figure IIB). Within the *ACE2*$^{-/y}$-Akita, the enrichment of several L-lysine biosynthesis pathways is observed. We next asked which bacterial taxa contributed to pathways involved in peptidoglycan biosynthesis. Surprisingly and consistently, *Bifidobacterium animalis* is the dominant species and is responsible for all peptidoglycan-related pathways in the double mutant mice (Figure 1E and 1F).

Loss of ACE2 Exacerbates Diabetes Mellitus-Mediated Disruption of the Gut Epithelial and Endothelial Barriers and Increases Peptidoglycan Translocation into the Circulation

Both the gut epithelial and endothelial barriers inhibit entry of microbial antigens into the bloodstream.[38] We next examined the integrity of the gut barrier in mice presenting with diabetes mellitus and ACE2 deficiency. The major expression site of ACE2 in the gut is the luminal surface of small intestinal epithelial cells, whereas lower ACE2 expression is observed in crypt cells and colon.[39] Therefore, for this study, we analyzed the gut barrier integrity in both the jejunum and ileum of the SI. Morphological analysis of the SI (ileum) showed no change in villi length in Akita or *ACE2*$^{-/y}$-Akita mice compared with their nondiabetic littermates (Figure 2A and 2B). However, *ACE2*$^{-/y}$-Akita mice showed a reduction of crypt depth (Figure 2C), decreased mucin expression, as supported by a reduced number of goblet cells (Figure 2D), and reduced muscular thickness (Figure 2E).

PV-1 (plasmalemma vesicle-associated protein-1) is considered a marker of endothelial cell permeability in both the brain-blood barrier and GVB.[38,40,41] In Figure 2F and 2G, we show that the expression of PV-1 was increased 2.7-fold in the lamina propria layer of the SI of Akita mice when compared with age-matched controls. The loss of ACE2 further increased the expression of this permeability marker. To assess GVB integrity, VE-cadherin was examined in the vasculature of the SI. Akita mice showed a significant decrease (≈40%) in VE-cadherin expression in the lamina propria layer of the SI when compared with nondiabetic groups (Figure 2H and 2I). ACE2 deficiency further exacerbated the diabetes mellitus-mediated reduction of VE-cadherin (≈41%) as compared to Akita alone (Figure 2I). Collectively, this data suggests that ACE2 plays an essential role in the diabetes mellitus-mediated disruption of the GVB.

Impaired GVB and increased permeability provide an opportunity for gut microbial antigens to cross the gut barrier and cause deleterious systemic effects. As we found increased biosynthesis of the bacterial antigen peptidoglycan in the fecal bacteria of *ACE2*$^{-/y}$-Akita mice, we next tested whether the disrupted GVB resulted in the translocation of peptidoglycan into the circulation. Consistent with the metatranscriptomic analysis, a nearly 3-fold increase of plasma peptidoglycan levels was detected in the *ACE2*$^{-/y}$-Akita mice when measured by ELISA (Figure 2J).

We next investigated whether peptidoglycan was similarly increased in diabetic individuals. Consistent with our findings in mice, plasma levels of peptidoglycan were increased (≈2-fold) in both T1D (P=0.0001) and T2D (P=0.0001) subjects when compared with nondiabetic controls (Figure 2K). Clinical data on the study subjects are included in Online Table I. Notably, FABP-2 (intestinal fatty acid-binding protein 2), a biomarker of gut epithelium tight junction barrier integrity, reportedly upregulated and released from the intestine in the presence of dysbiotic microbiota[42,43] was also elevated in the plasma of diabetic subjects compared with controls (Figure 2L).

ACE2 Deficiency Affects the Infiltration of MACs but not Proinflammatory and Immune Cells Into the Gut

BM-derived cells migrate to the gut and impact its function.[44,45] Thus, we evaluated whether the impaired integrity of the gut barrier in diabetic mice was associated with changes in the number of infiltrating cells. Diabetes mellitus did not affect the percentages of T cells (CD45$^+$CD3$^+$NK1.1$^-$; Figure 3A) or NK cells (CD45$^+$NK1.1$^+$CD3$^-$; Figure 3B) in the SI. The presence of diabetes mellitus did not change the percentages

Downloaded from http://ahajournals.org by on August 26, 2021

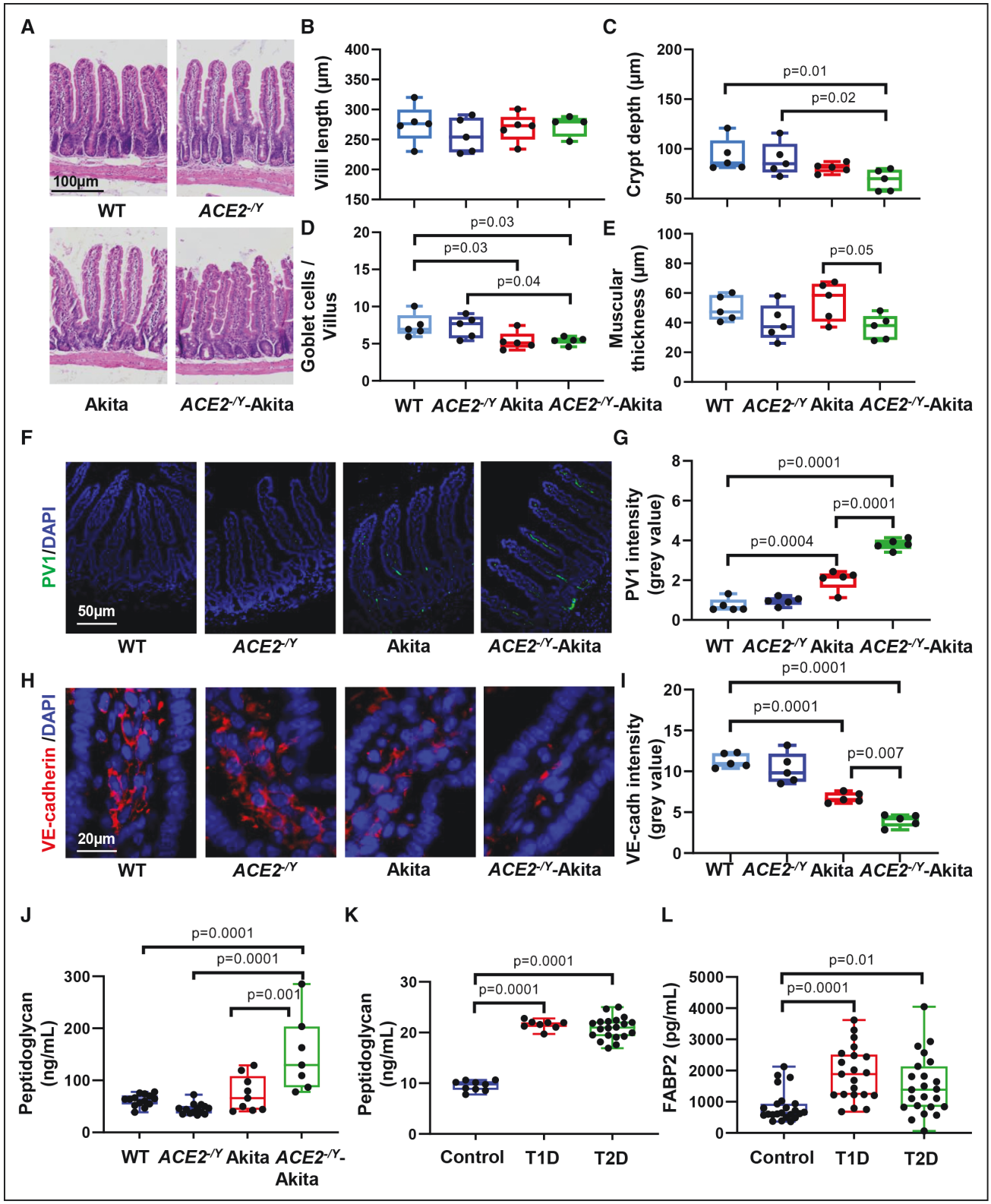

Figure 2. ACE2 (angiotensin-converting enzyme 2) deficiency worsened diabetes mellitus-induced disruption of the gut vascular barrier, causing the translocation of peptidoglycan (PGN) into the bloodstream.

A, Representative H&E staining images of ileum from diabetic and nondiabetic mice. **B**–**E**, No change was observed in villi length (**B**) among all 4 different groups, while reduced crypt depth (n=5 wild type [WT], *ACE2*$^{-/y}$, and Akita; 4 *ACE2*$^{-/y}$-Akita). **C**, Reduced numbers of goblet cells (*P*=0.01 and *P*=0.02; n=5). **D** Reduced muscular thickness (*P*=0.03 and *P*=0.04; n=5) (**E**) were observed in the *ACE2*$^{-/y}$-Akita mice (*P*=0.05) (n=5). **F**, Representative immunofluorescence images of permeability marker, PV-1 (plasmalemma vesicle-associated protein-1; green) staining. **G**, Quantitative data demonstrated that loss of ACE2 further increased the diabetes mellitus-induced elevation of PV-1 expression (*Continued*)

Downloaded from http://ahajournals.org by on August 26, 2021

of Ly6C$^+$ monocytes (CD45$^+$NK1.1$^-$CD3$^-$/Ly6G$^-$/CD115$^+$CD11b$^+$/Ly6C$^+$; Figure 3C) or Ly6C$^-$ monocytes (CD45$^+$NK1.1$^-$CD3$^-$/Ly6G$^-$/CD115$^+$CD11b$^+$/Ly6C$^+$; Figure 3D) in the gut.

To assess changes in vascular reparative cells, we examined MAC (CD45$^+$CD31$^+$Flk1$^+$) levels in the BM (Figure 3E and 3G) and SI (Figure 3F and 3H) of all 4 cohorts. Interestingly, MACs in the SI were decreased in *ACE2*$^{-/y}$, Akita, and *ACE2*$^{-/y}$-Akita mice, but no reduction in their levels was observed in the BM of these cohorts.

Administration of MACs Restores Gut Barrier Integrity

MACs represent a BM-derived population that have angiogenic potential, providing vascular repair by trophic support to the resident vasculature. These cells do not directly incorporate into vessels but associate in the proximity of an injured area[24] and release growth factors. We asked whether exogenous administration of MACs, CD45$^+$ CD31$^+$ Flk-1$^+$ cells could restore the integrity of the diabetic gut epithelium and GVB and prevent bacterial entry into the circulation. For these studies, MAC administration was given via the intraperitoneal route which represents the safest route of administration reducing the risk of clumping and obstruction in the lung capillaries.[46,47] MACs were isolated from the BM of healthy control (C57BL/6) mice, and 50 000 cells/mouse were injected 3 times every other day over 6 days into the 4 cohorts (WT, *ACE2*$^{-/y}$, Akita, and *ACE2*$^{-/y}$-Akita).

To monitor the integrity of the gut barrier, we examined the levels of protein expression for ZO-1 (Zonula occludens-1), an epithelial tight junction protein, and p120-catenin, a regulator of adherens junction stability, using immunohistochemistry. Decreased protein expression of ZO-1 has been associated with the loss of the epithelial barrier characteristics.[48] Three treatments with MACs over the 6-day period markedly increased the protein expression level of ZO-1 (Figure 4A and 4B) in the *ACE2*$^{-/y}$-Akita mice. p120-catenin was similarly increased in these mice subjected to MAC injections (Figure 4C and 4D).

We next determined whether MAC treatment affects the protein expression level of the endothelial permeability marker, PV-1, in Akita and *ACE2*$^{-/y}$-Akita mice. Consistent with our previous experiment, the PV-1 protein expression level was increased in the lamina propria layer in the both jejunum (Figure 5A and 5B) and ileum (Online Figure IIIA; Figure 5C) of saline-injected Akita and *ACE2*$^{-/y}$-Akita mice compared with WT and *ACE2*$^{-/y}$ mice. Treatment with MACs (3 injections over a 1-week period) markedly reduced the expression of PV-1 in Akita and *ACE2*$^{-/y}$-Akita mice (Figure 5A through 5C, Online Figure IIIA). MAC administration improved VE-cadherin expression in the blood vessels of the lamina propria layer in both the jejunum (Figure 5D and 5E) and ileum (Online Figure IIIB; Figure 5F) in Akita and *ACE2*$^{-/y}$-Akita mice, but significance was not achieved.

YAP (Yes-associated protein), a transcription factor of VE-Cadherin, mediates VE-cadherin-associated signaling and contributes to organizational modification of the adherens junctional complex and plays a role in vascular homeostasis. Loss of YAP results in less stable vessels and increased permeability.[49–51] The levels of YAP expression were restored in ileum and jejunum in Akita and in *ACE2*$^{-/y}$-Akita mice treated with MACs compared with PBS-treated Akita and *ACE2*$^{-/y}$-Akita mice (Figure 6A through 6D). Consequently, plasma levels of peptidoglycan were also reduced after MAC treatment as compared to PBS controls in both Akita (≈66% reduction) and *ACE2*$^{-/y}$-Akita cohorts (≈77% reduction; Figure 6E). Levels of zonulin were similarly reduced in the Akita and *ACE2*$^{-/y}$-Akita cohorts receiving MACs (Figure 6F). Together, these results support that the administration of MACs restored the GVB.

MAC Administration Beneficially Alters the Microbiome of the ACE2$^{-/y}$-Akita Mice

The microbiome of the *ACE2*$^{-/y}$, Akita, and *ACE2*$^{-/y}$-Akita mice treated with MACs showed changes in β-diversity (Online Figure IVA through IVC), revealing differential clustering between saline (control) and MAC-treated mice (permanova P=0.035) based on the expressed functional gene profile within each sample. A heat map displaying the differential abundances of the prominent taxa is presented in Online Figure IVD. Within the *ACE2*$^{-/y}$-Akita mice, we observed an absence of *B animalis* in MAC-treated mice. Downstream enrichment analyses were then conducted to determine if these shifts were theoretically beneficial or harmful to the mouse host (Online Figure IVE through IVG). Differential pathway analysis revealed a significant decrease in genes associated with peptidoglycan biosynthesis (P=0.05; Online Figure IVE), whereas an increase in gene expression associated with glutathione metabolism (with increased expression of Leucine aminopeptidase) and synthesis within MAC-treated *ACE2*$^{-/y}$-Akita in comparison to *ACE2*$^{-/y}$-Akita saline samples (Online Figures IVF and V). A significant decrease in genes mapped to the methane

Figure 2 Continued. level in the lamina propria (LP; P=0.0004 and P=0.0001; n=5). **H**, Representative images and quantitative graph (**I**) showed that ACE2 depletion played a key role in the diabetes mellitus-caused reduction of VE-Cadherin (red) expression in the gut vascular barrier (P=0.007, P=0.0001; n=5). **J**, The level of circulating peptidoglycan was robustly increased in the *ACE2*$^{-/y}$-Akita mice (P=0.001, P=0.0001; n=14 WT; 14 *ACE2*$^{-/y}$; 9 Akita; and 7 *ACE2*$^{-/y}$-Akita). **K**, The level of circulating peptidoglycan (P=0.0001) (n=9 control; 8 type 1 diabetes mellitus [T1D]; and 20 type 2 diabetes mellitus [T2D]) and (**L**) levels of FABP-2 (intestinal fatty acid-binding protein; P=0.01, P=0.0001; n=23 control; 21 T1D; and 23 T2D) in diabetic subjects vs controls. One-way ANOVA.

Downloaded from http://ahajournals.org by on August 26, 2021

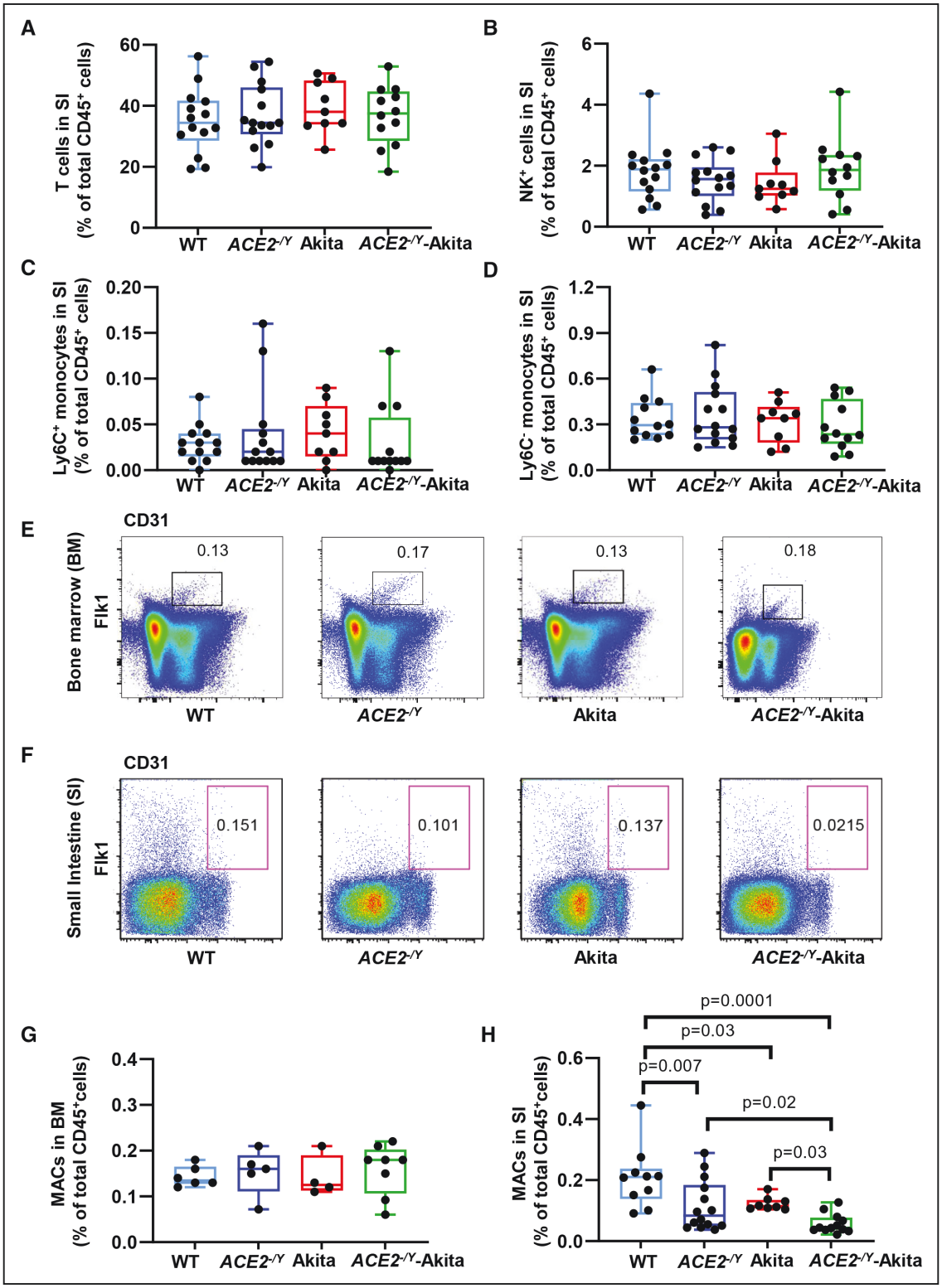

Figure 3. Loss of ACE2 (angiotensin-converting enzyme 2) worsens diabetes mellitus-induced reduced infiltration of bone marrow (BM)-derived myeloid angiogenic cells (MACs) into the small intestine, without affecting proinflammatory and immune cell types. No differences of phenotypic (**A**) T cells (n=14 wild type [WT]; 14 *ACE2*$^{-/y}$; 9 Akita; and 12 *ACE2*$^{-/y}$-Akita), (**B**) natural killer (NK) cells (n=14 WT; 14 *ACE2*$^{-/y}$; 9 Akita; and 12 *ACE2*$^{-/y}$-Akita), (**C**) Ly6C^{+} monocytes (n=13 WT; 13 *ACE2*$^{-/y}$; 9 Akita; and 12 *ACE2*$^{-/y}$-Akita), and (**D**) Ly6C^{-} monocyte (n=12 WT; 14 *ACE2*$^{-/y}$; 9 Akita; and 12 *ACE2*$^{-/y}$-Akita) in the small intestine lamina propria (LP) layer among the 4 different cohorts. **E**, Representative flow data presenting MAC populations in cells obtained from BM of each group and (**F**) LP of the small intestine. **G**, Quantitative data of percentage of MACs (CD45^{+}CD31^{+}Flk-1^{+}) in BM show no difference between the 4 cohorts (n=6 WT; 5 *ACE2*$^{-/y}$; 4 Akita; and 8 *ACE2*$^{-/y}$-Akita); however, (**H**) MACs are reduced in the small intestine in the *ACE2*$^{-/y}$, Akita, and *ACE2*$^{-/y}$-Akita (P=0.02, P=0.03, P=0.007, P=0.0001) (n=10 WT; 14 *ACE2*$^{-/y}$; 8 Akita; and 12 *ACE2*$^{-/y}$-Akita). One-way ANOVA.

Downloaded from http://ahajournals.org by on August 26, 2021

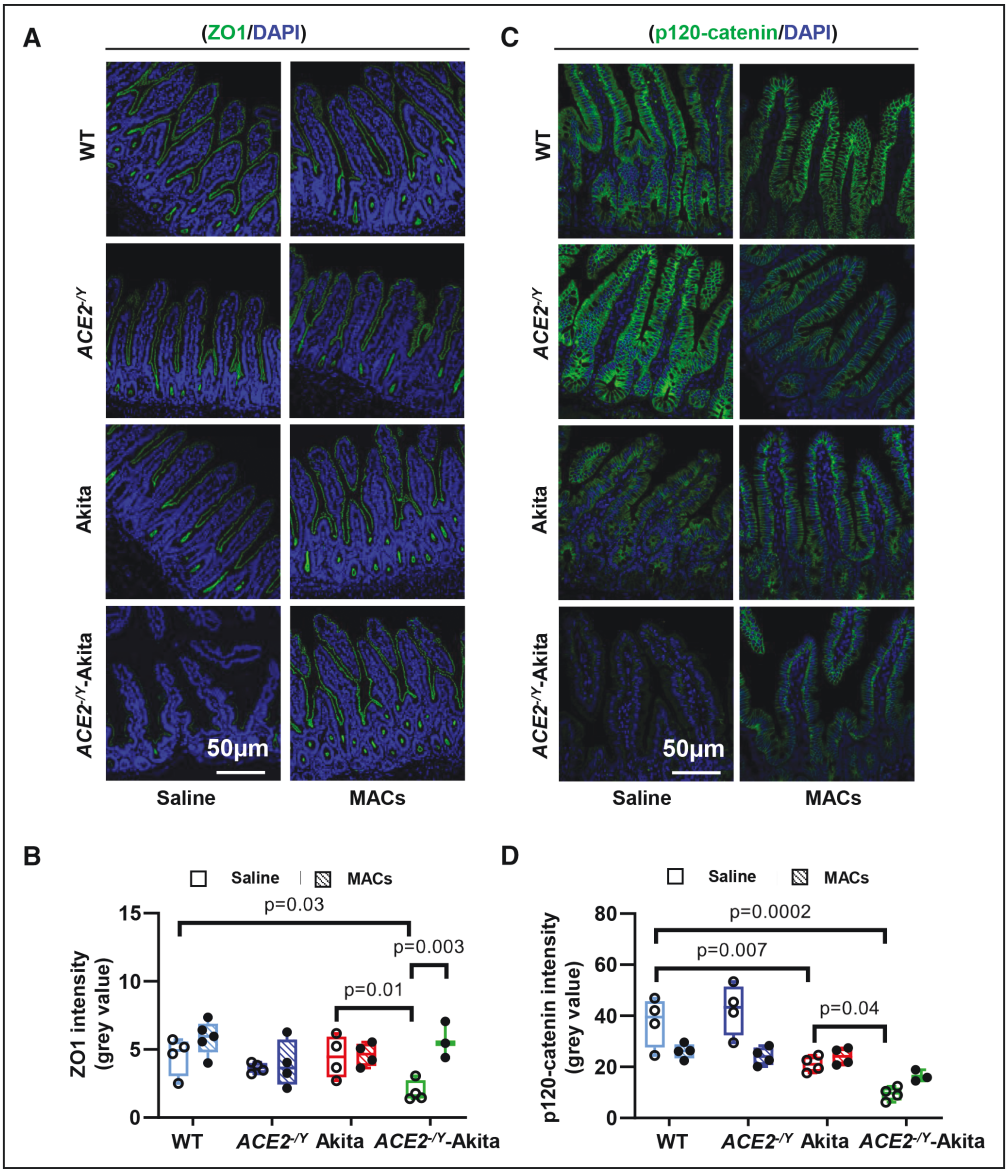

Figure 4. Myeloid angiogenic cells (MACs) treatment restored the gut epithelial integrity in *ACE2−/y*-Akita mice.
A–**C**, All 4 cohorts, wild type (WT), *ACE2*$^{-/y}$, Akita, and *ACE2*$^{-/y}$-Akita were treated 3 times over 6 days with either PBS control or MACs sorted from healthy mouse bone marrow. **A**, Representative images of ZO-1 (Zonula occludens-1) staining (green) in saline-treated controls or MAC-treated groups (ileum). **B**, Quantitative graphs showed that MAC treatment corrected the reduced expression of ZO-1 in the ileum (P=0.01, P=0.03, and P=0.003; n=3–5). **C**, Representative images of p120-catenin staining (green) in saline-treated controls or MAC treatment groups (ileum). **D**, Quantitative graphs showed that MAC treatment prevented diabetes mellitus-mediated reduction of p-120-catenin (P=0.04, P=0.007, and P=0.0002; n=3–4). One-way ANOVA.

metabolism was observed in MAC-treated *ACE2*$^{-/y}$-Akita mice compared with saline-injected *ACE2*$^{-/y}$-Akita mice with increase of genes that lead to D-Fructose production (Online Figures IVG and VI).

Peptidoglycan Treatment Does not Affect Inflammasome Activation in HRECs

Peptidoglycan and lipopolysaccharide are both well known as bacterial-derived stimuli that drive systemic inflammatory responses. The upregulation of circulating lipopolysaccharide poses an important interaction between the progression of microvascular complications and inflammation.[52] However, little is known about the contribution of peptidoglycan to these complications, in particular diabetic retinopathy. Both human and murine circulating monocytes responded to peptidoglycan stimulation with release of proinflammatory cytokines such as IL (interleukin)-1β in an Nlrp3 inflammasome and caspase-1 dependent manner (Online Figure VIIA through VIIE). However, neither IL-1β nor IL-18 were detected in HRECs after peptidoglycan treatment, suggesting that peptidoglycan is not an effective ligand of inflammasome activation in HRECs (Online Figure VIIF).

Downloaded from http://ahajournals.org by on August 26, 2021

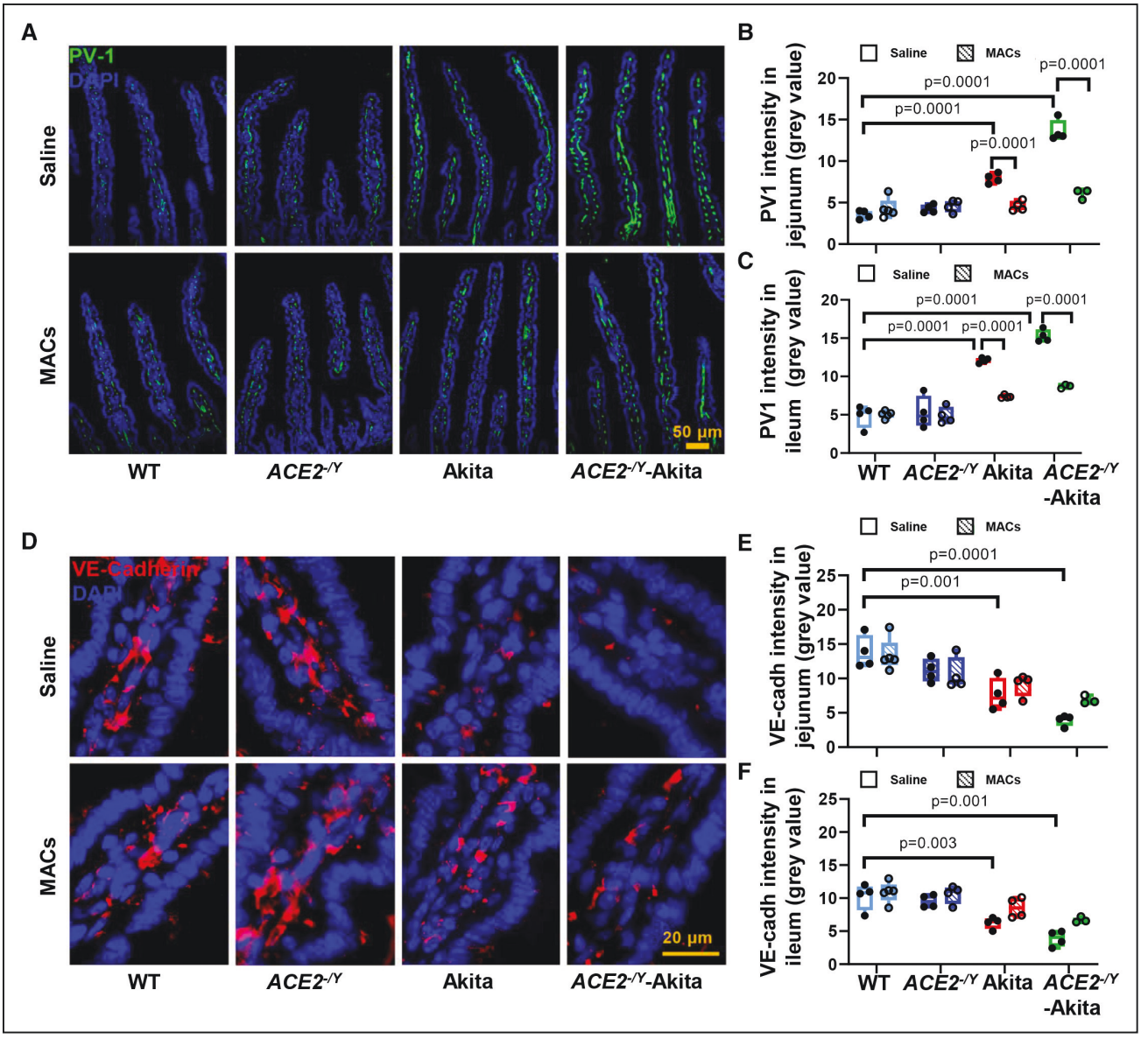

Figure 5. Myeloid angiogenic cells (MACs) treatment restored the gut vascular integrity in *ACE2–/y*-Akita mice.
A–**C**, Diabetic and nondiabetic mice were treated for 6 d with either PBS control or MACs sorted from healthy mouse bone marrow. **A**, Representative images of PV-1 (plasmalemma vesicle-associated protein-1) staining (green) in saline control-treated groups or MAC treatment groups (jejunum). **B** and **C**, Quantitative graphs showed that MAC treatment corrected the diabetes mellitus-induced expression of PV-1 in both jejunum (P=0.0001) (**B**), and ileum (P=0.0001) (**C**) (n=3–5). **D**, Representative images of VE-cadherin staining (red) in control or MAC treatment groups (jejunum). **E** and **F**, Quantitative graphs showed that MAC treatment prevented diabetes mellitus-mediated reduction of VE-cadherin expression in both jejunum (P=0.001, P=0.0001) (**E**), and ileum (P=0.001, P=0.003) (**F**) (n=3–5). One-way ANOVA.

Peptidoglycan Treatment Activates TLR-2 Mediated MyD88/ARNO/ARF6 Signaling in HRECs

TLR-2 can recognize bacterial cell wall components and is expressed by retinal endothelial cells.[53] To investigate whether peptidoglycan can increase TLR-2 expression, HRECs were treated with peptidoglycan (40 and 100 μg/mL) for 24 hours, and TLR-2 expression was assessed by changes in immunofluorescence (Figure 7A and 7B) and flow cytometry (Figure 7C and 7D). Peptidoglycan treatment resulted in increased TLR-2 immunofluorescence (P=0.0001) which were confirmed using flow cytometry that demonstrated an increase in surface TLR-2 (P=0.01) in the peptidoglycan-treated group compared with untreated cells (Figure 7C and 7D). Glucose (25 mmol/L) treated HRECs were used as a positive control for TLR-2 activation and mannitol (25 mmol/L) as a positive control for osmolarity. Due to the greater effect of peptidoglycan on TLR-2 expression at the dose of 100 μg/mL, this concentration was used in all subsequent experiments.

TLR-2 activation requires the recruitment of MyD88. Increased cytoplasmic expression of MyD88 was

Downloaded from http://ahajournals.org by on August 26, 2021

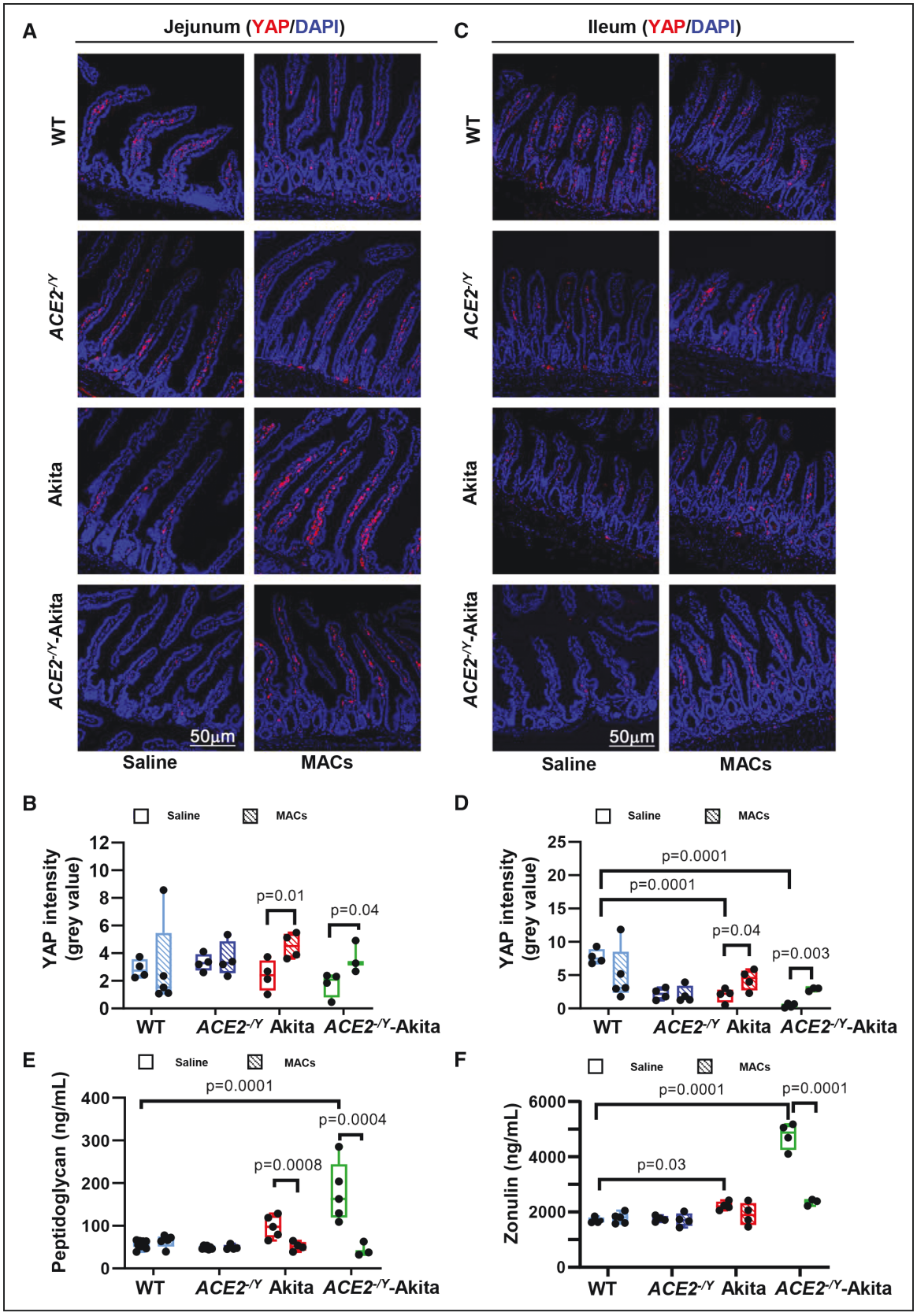

Figure 6. Myeloid angiogenic cell (MAC) treatment restored YAP (Yes-associated protein) expression in the gut and re-established vascular integrity to prevent the translocation of peptidoglycan in diabetes mellitus.
A, Representative images of YAP immunofluorescence staining in the jejunum. **B**, YAP expression (red) is increased by MAC treatment in the *Akita* and *ACE2*$^{-/y}$-Akita mice (P=0.01, P=0.04) (n=3–5). **C**, Representative images of YAP immunofluorescence staining in the ileum. (*Continued*)

Downloaded from http://ahajournals.org by on August 26, 2021

observed in peptidoglycan-treated cells as compared with untreated cells with expression being almost 3-fold higher (P=0.005) in peptidoglycan-treated cells (Figure 7E and 7F). MyD88 stimulates ARNO and ARF6, a member of the family of small GTPases, to promote vascular permeability.[54,55] Immunofluorescence staining revealed that peptidoglycan treatment significantly increased ARNO (P=0.001; Figure 7E and 7F) and ARF6 expression (2-fold, P=0.0001; Figure 7E and 7F) in HRECs.

Peptidoglycan Treatment Destabilized p120-Catenin, Promoting Adherens Junction Disruption, While NAV2729 (ARF6 Inhibitor) Blocked the Effect of Peptidoglycan, Restoring Adherens Junction Integrity

Destabilization of p120-catenin results in failure to form compact adherens junction connections and reduces barrier function[56] by internalization of VE-cadherin. We next examined whether peptidoglycan-mediated vascular leakage is associated with peptidoglycan-mediated activation of MyD88/ARNO/ARF6 signaling through destabilization of p120-catenin and internalization of VE-cadherin. After peptidoglycan treatment, the plasma membrane localization of p120-catenin was decreased in HRECs (arrowheads, P=0.009, Figure 7G and 7H). The reduction of p120-catenin turnover was further confirmed by western blot analysis (P=0.05; Figure 7I and 7J). In the adherens junctional complex, p120-catenin binds with the cytoplasmic tail of VE-cadherin and stabilizes the membrane localization of VE-cadherin to maintain barrier integrity. With the loss of p120-catenin, the integrity of adherens junctions in HRECs was lost, as observed by decreased VE-cadherin expression (P=0.005; Figure 7I and 7K).

To confirm the functional role of ARF6 in vascular damage, HRECs were treated for 1 hour with NAV2729 (an inhibitor of ARF6, 10 µmol/L) before cotreatment with peptidoglycan for 24 hours. NAV2729 treatment maintained p120-catenin localization in the plasma membrane (Figure 7G through 7J) and supported the restoration of adherens junctions through increased VE-cadherin expression (Figure 7I and 7K). These results establish that peptidoglycan-mediated activation of ARF6 plays an essential role in enhancing endothelial permeability in the retina. Furthermore, deactivation of ARF6 improves endothelial barrier integrity and reduces vascular leakage.

DISCUSSION

In this study, we found that disruption of the gut barrier in *ACE2*$^{-/y}$, Akita, and *ACE2*$^{-/y}$-Akita mice resulted from a loss of MACs, a population of hematopoietic cells previously defined by the surface markers CD45^{+}CD31^{+}Flk1^{+}[29]. This population of hematopoietic cells was markely reduced in the SI of the *ACE2*$^{-/y}$, Akita, and *ACE2*$^{-/y}$-Akita cohorts, suggesting that the loss of MACs was likely responsible for the barrier dysfunction and endotoxemia observed in these cohorts. Consistently, the exogenous administration of MACs restored the functional and anatomic integrity of the GVB and decreased the levels of peptidoglycan in the circulation of these mice. These results support the notion that loss of protective renin-angiotensin system results in the dysregulation of the BM-gut axis, a defect that is intensified in the presence of T1D. In turn, BM dysfunction contributes to increased gut epithelial and endothelial cell permeability and peptidoglycan levels in the circulation by reducing the production of this key reparative population, MACs. peptidoglycan, which is increased in the gut and ultimately enters the circulation, originates from bacterial species with increased peptidoglycan gene expression. Importantly, we observed increased peptidoglycan levels in the circulation of the *ACE2*$^{-/y}$, Akita, and *ACE2*$^{-/y}$-Akita mice with the highest levels in the *ACE2*$^{-/y}$-Akita mice. We also demonstrated that exogenous administration of MACs directly impacted the species composition of the microbiome and their gene production. The microbiome of the *ACE2*$^{-/y}$-Akita mice injected with MACs demonstrated the most profound changes including reduction of peptidoglycan biosynthesis pathways, reduced methane metabolism, and increased glutathione metabolism.

In healthy tissue, damage is balanced by physiological repair. Hematopoietic cells such as MACs also termed early endothelial progenitor cells[31,57,58] or circulating angiogenic cells.[59–64] MACs[24] possess angioge25nic and vascular repair capacity via paracrine activity. MACs are recruited to injured or angiogenic sites and secrete regulatory cytokines and growth factors that promote vessel repair by local vascular wall resident progenitor cells. MACs were first generated through the culture of peripheral blood mononuclear cells in endothelial cell-selective medium containing VEGF (vascular endothelial growth factor) for 4 to 7 days.[26,33,65] In diseases such as diabetes mellitus, coronary artery disease, and hypertension, reduced levels and function of these cells[28,66] is observed. Ward et al reported that MACs from subjects with cardiovascular disease exhibited reduced migration towards VEGF compared with cells from healthy controls. Tepper et al[33] showed that MACs from type 2 diabetics

Figure 6 Continued. **D**, YAP expression is increased by MAC treatment in the *Akita* and *ACE2*$^{-/y}$-Akita mice (P=0.04, P=0.003, P=0.0001) (n=3–5). **E**, Peptidoglycan (P=0.0001, P=0.0004, P=0.0008; saline n=10 wild type [WT]; 7 *ACE2*$^{-/y}$; 5 Akita; and 5 *ACE2*$^{-/y}$-Akita: MACs-treated groups n=3–5) and (**F**) zonulin (P=0.03, P=0.0001; n=3–5) levels were increased in the same cohort of diabetic mice and largely reduced by MAC treatment in both Akita and *ACE2*$^{-/y}$-Akita mice. One-way ANOVA. DAPI (4',6-diamidino-2-phenyllindole) was used for nuclear staining (blue).

Downloaded from http://ahajournals.org by on August 26, 2021

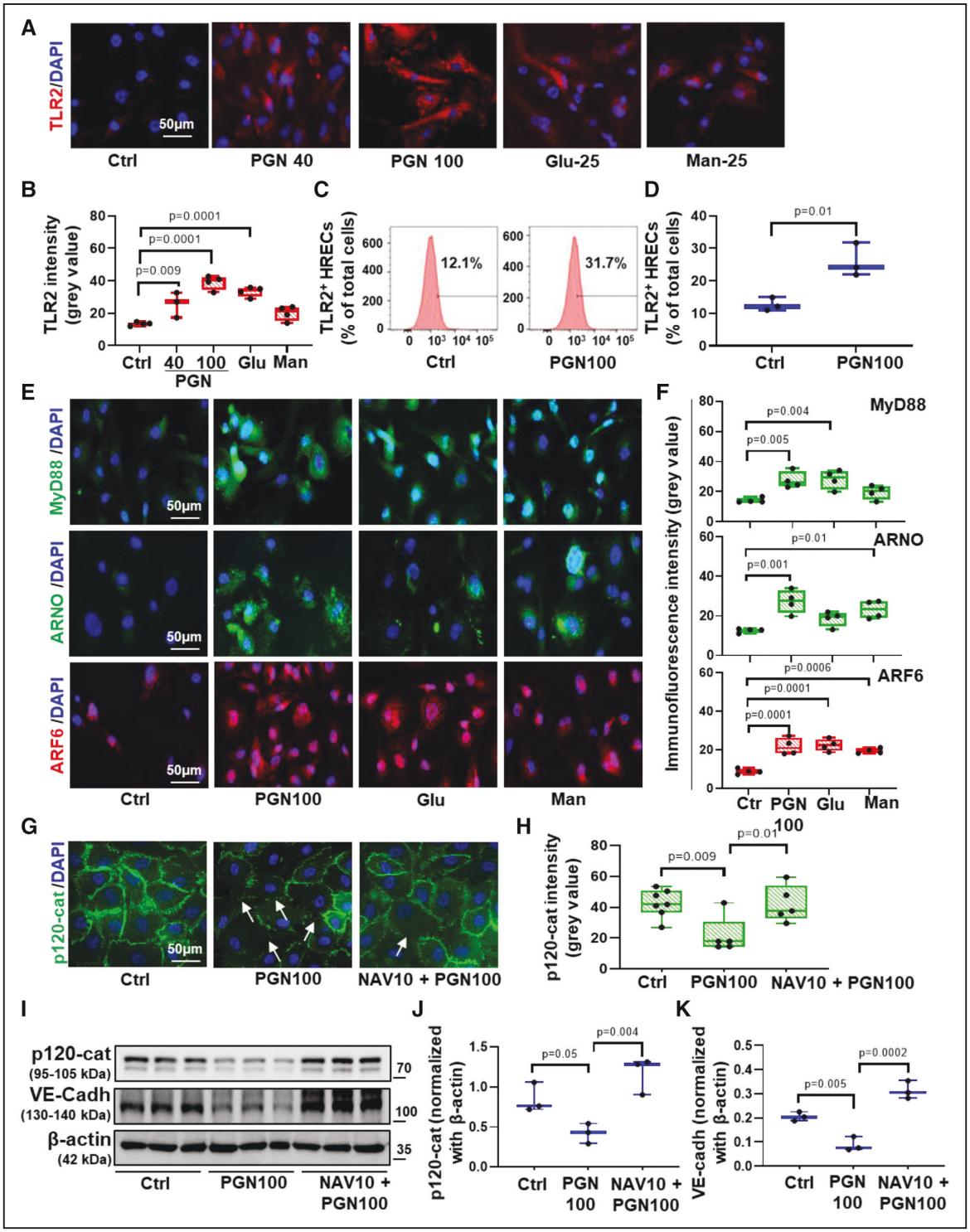

Figure 7. Peptidoglycan (PGN) treatment increased vascular permeability via TLR-2 (Toll-like receptor 2)-mediated activation of the MyD88 (myeloid differentiation primary response protein 88)/ARNO (ADP-ribosylation factor nucleotide-binding site opener)/ARF6 (ADP-ribosylation factor 6) signaling cascade.

HRECs (human retinal endothelial cells) were treated with PGN (40 and 100 μg/mL) for 24 h. The expression of TLR-2 (red) was examined by immunofluorescence (**A**) and quantitated (*P*=0.009, *P*=0.0001; n=3–4) (**B**). **C** and **D**, Flow cytometry assessment of percentage of cells expressing TLR-2 (*P*=0.01) (n=3). **E** and **F**, PGN treatment enhanced the expression of MyD88 (green) (*P*=0.004, *P*=0.005), ARNO (green; *P*=0.01, *P*=0.001) and ARF6 (red) (*P*=0.0001, *P*=0.0006) in HRECs (n=4). Effect of PGN on p120-catenin (green) expression in HRECs with and without NAV2729 treatment was determined by immunofluorescence staining (*P*=0.01, *P*=0.009; n=5–7) (**G** and **H**) and Western blot analysis (*P*=0.05, *P*=0.004; n=3) (**I** and **J**). **I** and **K**, Western blot analysis of PGN treatment effect on VE-cadherin expression in HRECs (*P*=0.005, *P*=0.0002) (n=3). Glucose (25 mmol/L)-treated HRECs were used as a positive control; mannitol (25 mmol/L)-treated cells served as a positive control for osmolarity. One-way ANOVA and unpaired *t* test. DAPI (4',6-diamidino-2-phenyllindole) was used for nuclear staining (blue).

Downloaded from http://ahajournals.org by on August 26, 2021

had impaired proliferation and adhesion. Vasa et al[26] observed an inverse correlation between the number and migratory activity of MACs and risk factors for coronary artery disease. Thus, it is unsurprising that reduced levels of MACs were observed not only in the intestine of the diabetic mice but also in the intestines of the *ACE2*$^{-/y}$ and *ACE2*$^{-/y}$-Akita mice.

Thus, MAC quantity and function are robust biomarkers of vascular risk for a multitude of diseases, particularly vascular diseases. MACs can be distinguished from late out-growth cells or endothelial colony-forming cells (ECFCs), which are vascular wall-derived (not BM-derived), but none the less are present in the circulation as they slough off into the blood and are captured in peripheral blood samples. However, because both ECFCs of endothelial lineage and MACs of hematopoietic linage are present at sites of neovascularization and the cells co-express a host of similar surface markers, it is difficult to discriminate them form each other at sites of vascular repair and to appreciate their individual contribution to the healing or regenerative process. ECFCs were not used in our current studies but could represent an excellent alternative source of cells to directly replace dysfunctional endothelium in the GVB by forming cellular patches at the site of denuding injury in the gut.[67,68]

Despite the clinical importance and well-studied therapeutic role of MACs in cardiovascular diseases, peripheral vascular disease, and diabetes mellitus, there is still no consensus regarding the definition and definitive marker panels for MACs.[24] Several review articles have summarized the various cell surface marker combinations used to define the hematopoietic/MACs.[69,70] The vast majority of the literature has defined MACs using different combinations of hematopoietic markers (CD34 in humans and CD45 in murine) and endothelial markers, such as CD31, VEGFR2 (KDR [kinase insert domain receptor] in humans, Flk-1 in murine), CD133, VEGFR1, and Tie-2.[69,70] In our study, we used mouse hematopoietic marker CD45 in combination with angiogenic markers CD31 and Flk-1, as previously shown in Hyongbum's study.[29] Remarkably, the BM CD31$^+$ cells expressed various other angiogenic markers such as VEGFR2 and represented a highly angiogenic and vasculogenic cell population.

Because of the discrepancies in the field, it is noted that more systematic and standardized tests should be done in the future to harmonize the definition and standards for MAC populations. The field of vascular progenitors has additional confounders that must be considered, such as the response of the MACs or ECFCs is likely dependent on the animal model used to evaluate the cells, the genetic background of the mouse, the type of vascular injury incurred, the organ system being challenged, and the nature of the angiogenic stimulus. Thus, the behavior of MACs (and ECFCs) will likely be different depending on whether the cells are responding to a disturbed GVB, a tumor, a denuded artery, a myocardial infarction, ocular ischemia, or a traumatic injury.

A novel finding of our studies is the identification that peptidoglycan-dependent stimulation of TLR-2 in the vasculature does not result in activation of the inflammasome. Instead, it appears that the peptidoglycan-dependent vascular permeability occurs through TLR-2/MyD88/ARNO/ARF6 signaling pathway.[54,55,71,72] Thus, our studies support that peptidoglycan in the circulation can enhance retinal vascular permeability and likely permeability in other vascular beds. A central regulator of the adherens junctional complex, p120-catenin, is localized in the JMD (juxtamembrane domain) region of the cytoplasmic tail of VE-cadherin. The function of p120-catenin in the adherens junctional complex is to regulate cadherin stability at the plasma membrane. A growing body of evidence indicates that destabilization of p120-catenin results in failure to form compact adherens junction connections and results in reduced barrier function[56] owing to internalization of cadherin. We showed that peptidoglycan-mediated vascular leakage is associated with destabilization of p120-catenin and a significant reduction in membrane localization of p120-catenin after peptidoglycan treatment in HRECs. Small GTPases of the Rho family, primarily ARF6, are intimately involved in the regulation of this process. ARF6 regulates VE-cadherin/p120-catenin internalization.[73] We further confirmed the functional role of ARF6 in retinal damage by demonstrating that the inhibitor of ARF6 (NAV2729) restored adherens junctional integrity through increased p120-catenin expression, resulting in stabilized VE-Cadherin. These results establish that peptidoglycan-mediated activation of ARF6 plays an important role in enhancing endothelial permeability in the vasculature, including the retina, and deactivation of ARF6 by NAV2729 improves the endothelial barrier and reduces vascular leakage (Figure 8).

Several additional points should be considered. First, loss of MACs is not solely responsible for reduced barrier characteristics but also the loss of beneficial bacteria could adversely impact gut barrier function. Second, *Akkermansia muciniphila*[74–77] is typically considered a beneficial bacterium[78,79] that has been shown to be decreased in diabetes mellitus. However, there are reports including our own previously published study that support that *A muciniphila* is increased in diabetic mice.[1] In the current work, we observed an increase in *A muciniphila* in Akita mice but not in the *ACE2*$^{-/y}$-Akita group. We interpret the increase in *A muciniphila* as a compensation response. Considering this is the first microbiome study using Akita mice with 9 months of diabetes mellitus, it may also represent a unique feature of this mouse model. Furthermore, the levels of mucin, which we did not examine, impact the levels (and gene expression) of *A muciniphila* and may have influenced our findings. Third, metatranscriptomic analysis showed that *B animalis* was responsible for the peptidoglycan generation. While *B animalis* is typically

Downloaded from http://ahajournals.org by on August 26, 2021

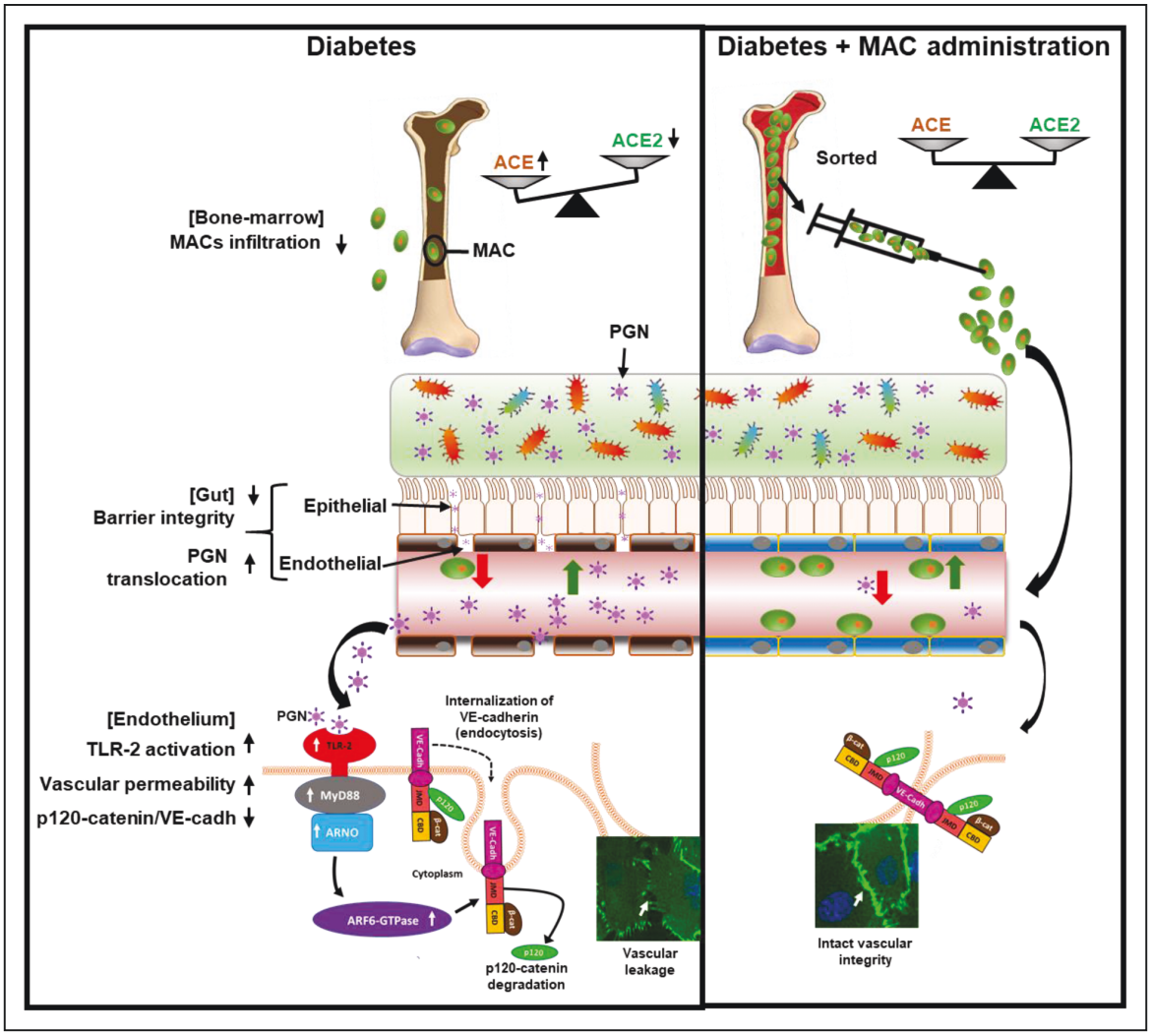

Figure 8. Schematic diagram showing the role of myeloid angiogenic cells (MACs) in maintaining gut barrier and preventing systemic effects of increased bacterial antigens.

We show that in diabetes mellitus, an imbalance of renin-angiotensin system (RAS; loss of ACE2 [angiotensin-converting enzyme 2]) results in reduced infiltration of MACs into the gut. The inadequate levels of MACs prevent repair of the gut barrier resulting in peptidoglycan (PGN) translocation into the circulation through the leaky gut. Circulating PGN binds to its receptor TLR-2 (Toll-like receptor 2), activating the MyD88 (myeloid differentiation primary response protein 88)/ARNO (ADP-ribosylation factor nucleotide-binding site opener)/ARF6 (ADP-ribosylation factor 6) signaling cascade. In endothelial cells, VE-cadherin, an adhesion molecule of adherens junction, plays a key role in regulating endothelial permeability. Adherens junctions are multiprotein complexes which consist of extracellular domains (VE-cadherins) and intracellular domains (p120-catenin: juxtamembrane domain; and β-catenin: catenin binding domain) to facilitate cell adhesive functions. Circulatory PGN mediated ARF6 signaling disassembles the adherens junctional complex through decreasing the p120-catenin turnover, leading to internalization of VE-cadherin through a vesicular endocytosis process, enhancing vascular permeability. Treatment of diabetic mice with MACs, isolated from the bone marrow (BM) of healthy mice, reduces dysbiosis and restores gut vascular integrity reducing the deleterious systemic effects of gut antigens such as PGN.

considered a beneficial bacterium, we interpret our findings as follows. Peptidoglycan synthesis is not harmful when peptidoglycan stays inside the SI and colon. However, in our cohorts, peptidoglycan was translocated into the systemic circulation via a disrupted gut barrier and reached target tissues where it activated TLR-2 and its downstream signaling pathway, thus becoming harmful.

MACs in humans are best characterized by the surface marker CD34.[80] Clinicaltrials.gov currently lists 686 studies that use MAC populations for the treatment of a wide range of ischemic conditions ranging from limb ischemia to myocardial infarction. In these clinical studies, the cells are either injected into the targeted vascular bed, for example, the coronaries, or injected into the systemic circulation. Even when administered directly into a dysfunctional vasculature, the cells redistribute throughout the entire vasculature, thus potentially impacting the GVB and gut epithelium. We can only speculate at this point that the clinical use of $CD34^+$ cells could restore the gut epithelial barrier and GVB reducing deleterious or proinflammatory gut microbial products that produce metabolic endotoxemia.

In summary, we show the dramatic impact of diabetes mellitus and the loss of ACE2 on the BM-gut axis.

Downloaded from http://ahajournals.org by on August 26, 2021

Metatranscriptome analysis directed our efforts to peptidoglycan-producing bacteria that promoted intestinal permeability and resulted in increased serum levels of peptidoglycan and zonulin. Importantly, exogenous administration of MACs restored both GVB and epithelial integrity and reduced leakage of microbial peptides into the circulation. Thus, a novel aspect of our study rests in the demonstration of the dependency of MAC function on maintaining the gut barrier function and that MAC administration beneficially impacts the gut microbiome correcting diabetes mellitus-induced dysbiosis. To our knowledge, this is the first study to identify the importance of MACs in maintaining gut barrier integrity. With the growing recognition of how the microbiome influences the physiology of the host, this newly found role of BM-derived MACs supports the consideration of therapeutic strategies to increase the mobilization of MACs into the circulation or, in diseases where there is a reduced production of these cells, by providing exogenous administration of allogeneic CD34$^+$ cells.

ARTICLE INFORMATION

Received July 23, 2019; revision received October 10, 2019; accepted October 13, 2019.

Affiliations

From the Department of Anatomy, Cell Biology and Physiology (Y.D., A.G.O.), Department of Ophthalmology, The Eugene and Marilyn Glick Eye Institute (D.F., E.B.), and Riley Hospital for Children, Pediatric Surgery (A.R.J., T.A.M.), Indiana University School of Medicine, Indianapolis; Department of Endocrinology, The Second Affiliated Hospital of Chongqing Medical University, China (Y.D.); Department of Ophthalmology and Visual Sciences (R.P., S.L.C., A.L.F.L., J.L.F., M.D., S.K.N., M.B.G.), University of Alabama at Birmingham; Department of Surgery (G.K.S., B.A., P.R.N.), Ohio State University, Wright Labs, LLC, Huntingdon, PA (R.L., J.W.); and Department of Medicine, University of Alberta, Mazankowski Alberta Heart Institute, Edmonton, Canada (G.Y.O.).

Sources of Funding

This study was supported by the National Institutes of Health Grants R01EY012601, R01EY028858, R01EY028037, R01EY025383 to M.B. Grant; T32HL134640-01 to M. Dupont; T32HL105349 to J.L. Floyd; R01HL115140 to A.G. Obukhov; and HL122505, HL137799 to P.R. Nagareddy. Canadian Institutes of Health Research (883612) and Heart and Stroke Foundation (55542) to G.Y. Oudit. Research to Prevent Blindness unrestricted grant awarded to Department of Ophthalmology and Visual Sciences at UAB.

Disclosures

None.

REFERENCES

1. Beli E, Yan Y, Moldovan L, Vieira CP, Gao R, Duan Y, Prasad R, Bhatwadekar A, White FA, Townsend SD, et al. Restructuring of the gut microbiome by intermittent fasting prevents retinopathy and prolongs survival in db/db mice. *Diabetes*. 2018;67:1867–1879. doi: 10.2337/db18-0158
2. Clermont A, Bursell SE, Feener EP. Role of the angiotensin II type 1 receptor in the pathogenesis of diabetic retinopathy: effects of blood pressure control and beyond. *J Hypertens Suppl*. 2006;24:S73–S80. doi: 10.1097/01.hjh.0000220410.69116.f8
3. Hayden MR, Sowers KM, Pulakat L, Joginpally T, Krueger B, Whaley-Connell A, Sowers JR. Possible mechanisms of local tissue renin-angiotensin system activation in the cardiorenal metabolic syndrome and type 2 diabetes mellitus. *Cardiorenal Med*. 2011;1:193–210. doi: 10.1159/000329926
4. Miller AG, Tan G, Binger KJ, Pickering RJ, Thomas MC, Nagaraj RH, Cooper ME, Wilkinson-Berka JL. Candesartan attenuates diabetic retinal vascular pathology by restoring glyoxalase-I function. *Diabetes*. 2010;59:3208–3215. doi: 10.2337/db10-0552
5. Rojas M, Zhang W, Lee DL, Romero MJ, Nguyen DT, Al-Shabrawey M, Tsai NT, Liou GI, Brands MW, Caldwell RW, et al. Role of IL-6 in angiotensin II-induced retinal vascular inflammation. *Invest Ophthalmol Vis Sci*. 2010;51:1709–1718. doi: 10.1167/iovs.09-3375
6. Saiki A, Ohira M, Endo K, Koide N, Oyama T, Murano T, Watanabe H, Miyashita Y, Shirai K. Circulating angiotensin II is associated with body fat accumulation and insulin resistance in obese subjects with type 2 diabetes mellitus. *Metabolism*. 2009;58:708–713. doi: 10.1016/j.metabol.2009.01.013
7. Silva KC, Rosales MA, Biswas SK, Lopes de Faria JB, Lopes de Faria JM. Diabetic retinal neurodegeneration is associated with mitochondrial oxidative stress and is improved by an angiotensin receptor blocker in a model combining hypertension and diabetes. *Diabetes*. 2009;58:1382–1390. doi: 10.2337/db09-0166
8. Wiecek A, Chudek J, Kokot F. Role of angiotensin II in the progression of diabetic nephropathy-therapeutic implications. *Nephrol Dial Transplant*. 2003;18 (suppl 5):v16–v20. doi: 10.1093/ndt/gfg1036
9. Wilkinson-Berka JL, Rana I, Armani R, Agrotis A. Reactive oxygen species, Nox and angiotensin II in angiogenesis: implications for retinopathy. *Clin Sci (Lond)*. 2013;124:597–615. doi: 10.1042/CS20120212
10. Dominguez JM 2nd, Hu P, Caballero S, Moldovan L, Verma A, Oudit GY, Li Q, Grant MB. Adeno-associated virus overexpression of angiotensin-converting enzyme-2 reverses diabetic retinopathy in type 1 diabetes in mice. *Am J Pathol*. 2016;186:1688–1700. doi: 10.1016/j.ajpath.2016.01.023
11. Jarajapu YP, Bhatwadekar AD, Caballero S, Hazra S, Shenoy V, Medina R, Kent D, Stitt AW, Thut C, Finney EM, et al. Activation of the ACE2/angiotensin-(1-7)/Mas receptor axis enhances the reparative function of dysfunctional diabetic endothelial progenitors. *Diabetes*. 2013;62:1258–1269. doi: 10.2337/db12-0808
12. Verma A, Shan Z, Lei B, Yuan L, Liu X, Nakagawa T, Grant MB, Lewin AS, Hauswirth WW, Raizada MK, et al. ACE2 and Ang-(1-7) confer protection against development of diabetic retinopathy. *Mol Ther*. 2012;20:28–36. doi: 10.1038/mt.2011.155
13. Patel VB, Bodiga S, Basu R, Das SK, Wang W, Wang Z, Lo J, Grant MB, Zhong J, Kassiri Z, et al. Loss of angiotensin-converting enzyme-2 exacerbates diabetic cardiovascular complications and leads to systolic and vascular dysfunction: a critical role of the angiotensin II/AT1 receptor axis. *Circ Res*. 2012;110:1322–1335. doi: 10.1161/CIRCRESAHA.112.268029
14. Patel VB, Parajuli N, Oudit GY. Role of angiotensin-converting enzyme 2 (ACE2) in diabetic cardiovascular complications. *Clin Sci (Lond)*. 2014;126:471–482. doi: 10.1042/CS20130344
15. Duan Y, Beli E, Li Calzi S, Quigley JL, Miller RC, Moldovan L, Feng D, Salazar TE, Hazra S, Al-Sabah J, et al. Loss of angiotensin-converting enzyme 2 exacerbates diabetic retinopathy by promoting bone marrow dysfunction. *Stem Cells*. 2018;36:1430–1440. doi: 10.1002/stem.2848
16. Balmer ML, Schürch CM, Saito Y, Geuking MB, Li H, Cuenca M, Kovtonyuk LV, McCoy KD, Hapfelmeier S, Ochsenbein AF, et al. Microbiota-derived compounds drive steady-state granulopoiesis via MyD88/TICAM signaling. *J Immunol*. 2014;193:5273–5283. doi: 10.4049/jimmunol.1400762
17. Ivanov II, Atarashi K, Manel N, Brodie EL, Shima T, Karaoz U, Wei D, Goldfarb KC, Santee CA, Lynch SV, et al. Induction of intestinal Th17 cells by segmented filamentous bacteria. *Cell*. 2009;139:485–498. doi: 10.1016/j.cell.2009.09.033
18. Khosravi A, Yáñez A, Price JG, Chow A, Merad M, Goodridge HS, Mazmanian SK. Gut microbiota promote hematopoiesis to control bacterial infection. *Cell Host Microbe*. 2014;15:374–381. doi: 10.1016/j.chom.2014.02.006
19. Fresno M, Alvarez R, Cuesta N. Toll-like receptors, inflammation, metabolism and obesity. *Arch Physiol Biochem*. 2011;117:151–164. doi: 10.3109/13813455.2011.562514
20. Lee YK, Menezes JS, Umesaki Y, Mazmanian SK. Proinflammatory T-cell responses to gut microbiota promote experimental autoimmune encephalomyelitis. *Proc Natl Acad Sci U S A*. 2011;108(suppl 1):4615–4622. doi: 10.1073/pnas.1000082107
21. Leoni G, Neumann PA, Sumagin R, Denning TL, Nusrat A. Wound repair: role of immune-epithelial interactions. *Mucosal Immunol*. 2015;8:959–968. doi: 10.1038/mi.2015.63
22. Urbich C, Aicher A, Heeschen C, Dernbach E, Hofmann WK, Zeiher AM, Dimmeler S. Soluble factors released by endothelial progenitor cells promote migration of endothelial cells and cardiac resident progenitor cells. *J Mol Cell Cardiol*. 2005;39:733–742. doi: 10.1016/j.yjmcc.2005.07.003
23. Medina RJ, O'Neill CL, O'Doherty TM, Knott H, Guduric-Fuchs J, Gardiner TA, Stitt AW. Myeloid angiogenic cells act as alternative M2 macrophages and modulate angiogenesis through interleukin-8. *Mol Med*. 2011;17:1045–1055. doi: 10.2119/molmed.2011.00129

Downloaded from http://ahajournals.org by on August 26, 2021

24. Medina RJ, Barber CL, Sabatier F, Dignat-George F, Melero-Martin JM, Khosrotehrani K, Ohneda O, Randi AM, Chan JKY, Yamaguchi T, et al. Endothelial progenitors: a consensus statement on nomenclature. *Stem Cells Transl Med*. 2017;6:1316–1320. doi: 10.1002/sctm.16-0360
25. Fadini GP, Sartore S, Albiero M, Baesso I, Murphy E, Menegolo M, Grego F, Vigili de Kreutzenberg S, Tiengo A, Agostini C, et al. Number and function of endothelial progenitor cells as a marker of severity for diabetic vasculopathy. *Arterioscler Thromb Vasc Biol*. 2006;26:2140–2146. doi: 10.1161/01.ATV.0000237750.44469.88
26. Vasa M, Fichtlscherer S, Aicher A, Adler K, Urbich C, Martin H, Zeiher AM, Dimmeler S. Number and migratory activity of circulating endothelial progenitor cells inversely correlate with risk factors for coronary artery disease. *Circ Res*. 2001;89:E1–E7. doi: 10.1161/hh1301.093953
27. Schmidt-Lucke C, Rössig L, Fichtlscherer S, Vasa M, Britten M, Kämper U, Dimmeler S, Zeiher AM. Reduced number of circulating endothelial progenitor cells predicts future cardiovascular events: proof of concept for the clinical importance of endogenous vascular repair. *Circulation*. 2005;111:2981–2987. doi: 10.1161/CIRCULATIONAHA.104.504340
28. Werner N, Kosiol S, Schiegl T, Ahlers P, Walenta K, Link A, Böhm M, Nickenig G. Circulating endothelial progenitor cells and cardiovascular outcomes. *N Engl J Med*. 2005;353:999–1007. doi: 10.1056/NEJMoa043814
29. Kim H, Cho HJ, Kim SW, Liu B, Choi YJ, Lee J, Sohn YD, Lee MY, Houge MA, Yoon YS. CD31+ cells represent highly angiogenic and vasculogenic cells in bone marrow: novel role of nonendothelial CD31+ cells in neovascularization and their therapeutic effects on ischemic vascular disease. *Circ Res*. 2010;107:602–614. doi: 10.1161/CIRCRESAHA.110.218396
30. Chambers SEJ, O'Neill CL, Guduric-Fuchs J, McLoughlin KJ, Liew A, Egan AM, O'Brien T, Stitt AW, Medina RJ. The vasoreparative function of myeloid angiogenic cells is impaired in diabetes through the induction of IL1β. *Stem Cells*. 2018;36:834–843. doi: 10.1002/stem.2810
31. Asahara T, Murohara T, Sullivan A, Silver M, van der Zee R, Li T, Witzenbichler B, Schatteman G, Isner JM. Isolation of putative progenitor endothelial cells for angiogenesis. *Science*. 1997;275:964–967. doi: 10.1126/science.275.5302.964
32. Fadini GP, Losordo D, Dimmeler S. Critical reevaluation of endothelial progenitor cell phenotypes for therapeutic and diagnostic use. *Circ Res*. 2012;110:624–637. doi: 10.1161/CIRCRESAHA.111.243386
33. Tepper OM, Galiano RD, Capla JM, Kalka C, Gagne PJ, Jacobowitz GR, Levine JP, Gurtner GC. Human endothelial progenitor cells from type II diabetics exhibit impaired proliferation, adhesion, and incorporation into vascular structures. *Circulation*. 2002;106:2781–2786. doi: 10.1161/01.cir.0000039526.42991.93
34. Loomans CJ, de Koning EJ, Staal FJ, Rookmaaker MB, Verseyden C, de Boer HC, Verhaar MC, Braam B, Rabelink TJ, van Zonneveld AJ. Endothelial progenitor cell dysfunction: a novel concept in the pathogenesis of vascular complications of type 1 diabetes. *Diabetes*. 2004;53:195–199. doi: 10.2337/diabetes.53.1.195
35. Sorrentino SA, Bahlmann FH, Besler C, Müller M, Schulz S, Kirchhoff N, Doerries C, Horváth T, Limbourg A, Limbourg F, et al. Oxidant stress impairs in vivo reendothelialization capacity of endothelial progenitor cells from patients with type 2 diabetes mellitus: restoration by the peroxisome proliferator-activated receptor-gamma agonist rosiglitazone. *Circulation*. 2007;116:163–173. doi: 10.1161/CIRCULATIONAHA.106.684381
36. Mahé F, Rognes T, Quince C, de Vargas C, Dunthorn M. Swarm v2: highly-scalable and high-resolution amplicon clustering. *PeerJ*. 2015;3:e1420. doi: 10.7717/peerj.1420
37. Segata N, Izard J, Waldron L, Gevers D, Miropolsky L, Garrett WS, Huttenhower C. Metagenomic biomarker discovery and explanation. *Genome Biol*. 2011;12:R60. doi: 10.1186/gb-2011-12-6-r60
38. Spadoni I, Zagato E, Bertocchi A, Paolinelli R, Hot E, Di Sabatino A, Caprioli F, Bottiglieri L, Oldani A, Viale G, et al. A gut-vascular barrier controls the systemic dissemination of bacteria. *Science*. 2015;350:830–834. doi: 10.1126/science.aad0135
39. Hashimoto T, Perlot T, Rehman A, Trichereau J, Ishiguro H, Paolino M, Sigl V, Hanada T, Hanada R, Lipinski S, et al. ACE2 links amino acid malnutrition to microbial ecology and intestinal inflammation. *Nature*. 2012;487:477–481. doi: 10.1038/nature11228
40. Polakis P. Formation of the blood-brain barrier: Wnt signaling seals the deal. *J Cell Biol*. 2008;183:371–373. doi: 10.1083/jcb.200810040
41. Wang Y, Rattner A, Zhou Y, Williams J, Smallwood PM, Nathans J. Norrin/Frizzled4 signaling in retinal vascular development and blood brain barrier plasticity. *Cell*. 2012;151:1332–1344. doi: 10.1016/j.cell.2012.10.042
42. Sturgeon C, Fasano A. Zonulin, a regulator of epithelial and endothelial barrier functions, and its involvement in chronic inflammatory diseases. *Tissue Barriers*. 2016;4:e1251384. doi: 10.1080/21688370.2016.1251384
43. Guerrant RL, Leite AM, Pinkerton R, Medeiros PH, Cavalcante PA, DeBoer M, Kosek M, Duggan C, Gewirtz A, Kagan JC, et al. Biomarkers of environmental enteropathy, inflammation, stunting, and impaired growth in children in Northeast Brazil. *PLoS One*. 2016;11:e0158772. doi: 10.1371/journal.pone.0158772
44. Bain CC, Bravo-Blas A, Scott CL, Perdiguero EG, Geissmann F, Henri S, Malissen B, Osborne LC, Artis D, Mowat AM. Constant replenishment from circulating monocytes maintains the macrophage pool in the intestine of adult mice. *Nat Immunol*. 2014;15:929–937. doi: 10.1038/ni.2967
45. De Schepper S, Verheijden S, Aguilera-Lizarraga J, Viola MF, Boesmans W, Stakenborg N, Voytyuk I, Schmidt I, Boeckx B, Dierckx de Casterlé I, et al. Self-maintaining gut macrophages are essential for intestinal homeostasis. *Cell*. 2018;175:400–415.e13. doi: 10.1016/j.cell.2018.07.048
46. Fischer UM, Harting MT, Jimenez F, Monzon-Posadas WO, Xue H, Savitz SI, Laine GA, Cox CS Jr. Pulmonary passage is a major obstacle for intravenous stem cell delivery: the pulmonary first-pass effect. *Stem Cells Dev*. 2009;18:683–692. doi: 10.1089/scd.2008.0253
47. Kean TJ, Lin P, Caplan AI, Dennis JE. MSCs: delivery routes and engraftment, cell-targeting strategies, and immune modulation. *Stem Cells Int*. 2013;2013:732742. doi: 10.1155/2013/732742
48. Vivinus-Nébot M, Frin-Mathy G, Bzioueche H, Dainese R, Bernard G, Anty R, Filippi J, Saint-Paul MC, Tulic MK, Verhasselt V, et al. Functional bowel symptoms in quiescent inflammatory bowel diseases: role of epithelial barrier disruption and low-grade inflammation. *Gut*. 2014;63:744–752. doi: 10.1136/gutjnl-2012-304066
49. Choi HJ, Kwon YG. Roles of YAP in mediating endothelial cell junctional stability and vascular remodeling. *BMB Rep*. 2015;48:429–430. doi: 10.5483/bmbrep.2015.48.8.146
50. Choi HJ, Zhang H, Park H, Choi KS, Lee HW, Agrawal V, Kim YM, Kwon YG. Yes-associated protein regulates endothelial cell contact-mediated expression of angiopoietin-2. *Nat Commun*. 2015;6:6943. doi: 10.1038/ncomms7943
51. Giampietro C. VE-cadherin complex plasticity: EPS8 and YAP play relay at adherens junctions. *Tissue Barriers*. 2016;4:e1232024. doi: 10.1080/21688370.2016.1232024
52. Mendiola AS, Garza R, Cardona SM, Mythen SA, Lira SA, Akassoglou K, Cardona AE. Fractalkine signaling attenuates perivascular clustering of microglia and fibrinogen leakage during systemic inflammation in mouse models of diabetic retinopathy. *Front Cell Neurosci*. 2016;10:303. doi: 10.3389/fncel.2016.00303
53. Stewart EA, Wei R, Branch MJ, Sidney LE, Amoaku WM. Expression of Toll-like receptors in human retinal and choroidal vascular endothelial cells. *Exp Eye Res*. 2015;138:114–123. doi: 10.1016/j.exer.2015.06.012
54. Davis CT, Zhu W, Gibson CC, Bowman-Kirigin JA, Sorensen L, Ling J, Sun H, Navankasattusas S, Li DY. ARF6 inhibition stabilizes the vasculature and enhances survival during endotoxic shock. *J Immunol*. 2014;192:6045–6052. doi: 10.4049/jimmunol.1400309
55. Zhu W, London NR, Gibson CC, Davis CT, Tong Z, Sorensen LK, Shi DS, Guo J, Smith MC, Grossmann AH, et al. Interleukin receptor activates a MYD88-ARNO-ARF6 cascade to disrupt vascular stability. *Nature*. 2012;492:252–255. doi: 10.1038/nature11603
56. Xiao K, Oas RG, Chiasson CM, Kowalczyk AP. Role of p120-catenin in cadherin trafficking. *Biochim Biophys Acta*. 2007;1773:8–16. doi: 10.1016/j.bbamcr.2006.07.005
57. Asahara T, Masuda H, Takahashi T, Kalka C, Pastore C, Silver M, Kearne M, Magner M, Isner JM. Bone marrow origin of endothelial progenitor cells responsible for postnatal vasculogenesis in physiological and pathological neovascularization. *Circ Res*. 1999;85:221–228. doi: 10.1161/01.res.85.3.221
58. Takahashi M, Nakamura T, Toba T, Kajiwara N, Kato H, Shimizu Y. Transplantation of endothelial progenitor cells into the lung to alleviate pulmonary hypertension in dogs. *Tissue Eng*. 2004;10:771–779. doi: 10.1089/1076327041348563
59. Everaert BR, Van Laere SJ, Lembrechts R, Hoymans VY, Timmermans JP, Vrints CJ. Identification of macrophage genotype and key biological pathways in circulating angiogenic cell transcriptome. *Stem Cells Int*. 2019;2019:9545261. doi: 10.1155/2019/9545261
60. Ziegelhoeffer T, Fernandez B, Kostin S, Heil M, Voswinckel R, Helisch A, Schaper W. Bone marrow-derived cells do not incorporate into the adult growing vasculature. *Circ Res*. 2004;94:230–238. doi: 10.1161/01.RES.0000110419.50982.1C
61. Fazel S, Cimini M, Chen L, Li S, Angoulvant D, Fedak P, Verma S, Weisel RD, Keating A, Li RK. Cardioprotective c-kit+ cells are from the bone marrow and regulate the myocardial balance of angiogenic cytokines. *J Clin Invest*. 2006;116:1865–1877. doi: 10.1172/JCI27019

Downloaded from http://ahajournals.org by on August 26, 2021

62. Stadtfeld M, Graf T. Assessing the role of hematopoietic plasticity for endothelial and hepatocyte development by non-invasive lineage tracing. *Development*. 2005;132:203–213. doi: 10.1242/dev.01558
63. Takakura N, Watanabe T, Suenobu S, Yamada Y, Noda T, Ito Y, Satake M, Suda T. A role for hematopoietic stem cells in promoting angiogenesis. *Cell*. 2000;102:199–209. doi: 10.1016/s0092-8674(00)00025-8
64. Heil M, Eitenmüller I, Schmitz-Rixen T, Schaper W. Arteriogenesis versus angiogenesis: similarities and differences. *J Cell Mol Med*. 2006;10:45–55. doi: 10.1111/j.1582-4934.2006.tb00290.x
65. Kalka C, Masuda H, Takahashi T, Gordon R, Tepper O, Gravereaux E, Pieczek A, Iwaguro H, Hayashi SI, Isner JM, et al. Vascular endothelial growth factor(165) gene transfer augments circulating endothelial progenitor cells in human subjects. *Circ Res*. 2000;86:1198–1202. doi: 10.1161/01.res.86.12.1198
66. Jarajapu YP, Hazra S, Segal M, Li Calzi S, LiCalzi S, Jadhao C, Jhadao C, Qian K, Mitter SK, Raizada MK, et al. Vasoreparative dysfunction of CD34+ cells in diabetic individuals involves hypoxic desensitization and impaired autocrine/paracrine mechanisms. *PLoS One*. 2014;9:e93965. doi: 10.1371/journal.pone.0093965
67. Mund JA, Estes ML, Yoder MC, Ingram DA Jr, Case J. Flow cytometric identification and functional characterization of immature and mature circulating endothelial cells. *Arterioscler Thromb Vasc Biol*. 2012;32:1045–1053. doi: 10.1161/ATVBAHA.111.244210
68. Mund JA, Ingram DA, Yoder MC, Case J. Endothelial progenitor cells and cardiovascular cell-based therapies. *Cytotherapy*. 2009;11:103–113. doi: 10.1080/14653240802714827
69. Rose JA, Erzurum S, Asosingh K. Biology and flow cytometry of proangiogenic hematopoietic progenitors cells. *Cytometry A*. 2015;87:5–19. doi: 10.1002/cyto.a.22596
70. Duong HT, Erzurum SC, Asosingh K. Pro-angiogenic hematopoietic progenitor cells and endothelial colony-forming cells in pathological angiogenesis of bronchial and pulmonary circulation. *Angiogenesis*. 2011;14:411–422. doi: 10.1007/s10456-011-9228-y
71. Akira S, Takeda K. Toll-like receptor signalling. *Nat Rev Immunol*. 2004;4:499–511. doi: 10.1038/nri1391
72. Rajamani U, Jialal I. Hyperglycemia induces toll-like receptor-2 and -4 expression and activity in human microvascular retinal endothelial cells: implications for diabetic retinopathy. *J Diabetes Res*. 2014;2014:790902. doi: 10.1155/2014/790902
73. Santy LC, Casanova JE. Activation of ARF6 by ARNO stimulates epithelial cell migration through downstream activation of both Rac1 and phospholipase D. *J Cell Biol*. 2001;154:599–610. doi: 10.1083/jcb.200104019
74. Dao MC, Everard A, Aron-Wisnewsky J, Sokolovska N, Prifti E, Verger EO, Kayser BD, Levenez F, Chilloux J, Hoyles L, et al; MICRO-Obes Consortium. Akkermansia muciniphila and improved metabolic health during a dietary intervention in obesity: relationship with gut microbiome richness and ecology. *Gut*. 2016;65:426–436. doi: 10.1136/gutjnl-2014-308778
75. Everard A, Belzer C, Geurts L, Ouwerkerk JP, Druart C, Bindels LB, Guiot Y, Derrien M, Muccioli GG, Delzenne NM, et al. Cross-talk between akkermansia muciniphila and intestinal epithelium controls diet-induced obesity. *Proc Natl Acad Sci U S A*. 2013;110:9066–9071. doi: 10.1073/pnas.1219451110
76. Muccioli GG, Naslain D, Bäckhed F, Reigstad CS, Lambert DM, Delzenne NM, Cani PD. The endocannabinoid system links gut microbiota to adipogenesis. *Mol Syst Biol*. 2010;6:392. doi: 10.1038/msb.2010.46
77. Cani PD. Crosstalk between the gut microbiota and the endocannabinoid system: impact on the gut barrier function and the adipose tissue. *Clin Microbiol Infect*. 2012;18(suppl 4):50–53. doi: 10.1111/j.1469-0691.2012.03866.x
78. Cani PD, de Vos WM. Next-generation beneficial microbes: the case of akkermansia muciniphila. *Front Microbiol*. 2017;8:1765. doi: 10.3389/fmicb.2017.01765
79. Naito Y, Uchiyama K, Takagi T. A next-generation beneficial microbe: akkermansia muciniphila. *J Clin Biochem Nutr*. 2018;63:33–35. doi: 10.3164/jcbn.18-57
80. Fadini GP, Rigato M, Cappellari R, Bonora BM, Avogaro A. Long-term prediction of cardiovascular outcomes by circulating CD34+ and CD34+CD133+ stem cells in patients with type 2 diabetes. *Diabetes Care*. 2017;40:125–131. doi: 10.2337/dc16-1755

Downloaded from http://ahajournals.org by on August 26, 2021